Wetland soil history shapes microbial community composition, while hydrologic disturbance alters greenhouse gas fluxes

Regina B. Bledsoe[1,2], Colin G. Finlay[1,*], Ariane L. Peralta[1]

1. Department of Biology, East Carolina University, Greenville, NC 27858, USA
2. NewLeaf Symbiotics, St. Louis, MO 63132, USA

*Corresponding author: telephone: +1 307.690.1734, e-mail: finlayc21@students.ecu.edu

Regina B. Bledsoe and Colin G. Finlay are co-first authors.

Open Research statement: All code and data used in this study are in a public GitHub repository (https://github.com/PeraltaLab/WetlandMesocosm_GHG_Timberlake) with a Zenodo DOI (https://doi.org/10.5281/zenodo.15528281). Raw amplicon sequence files can be found at NCBI SRA BioProject ID PRJNA636184, and metagenome sequence files can be found at NCBI SRA BioProject ID PRJNA641216.

Key words/phrases: 16S rRNA; carbon dioxide; denitrification; greenhouse gases; hydrology; metagenomics; methane; nitrous oxide; plant cover; plant-microbe interactions; soil mesocosms; soil redox

Abstract

While wetlands represent a small fraction (~5-10%) of the world's land surface, it is estimated that one-third of wetlands have been lost due to human activities. Wetland habitat loss decreases ecosystem benefits, including improved water quality and climate change mitigation. These microbially mediated functions are dependent on redox conditions, which are altered by soil hydrology and the presence of plants. We tested the overarching hypothesis that while microbial community composition would be resistant to change due to long-term hydrologic history, key functions like greenhouse gas production would remain plastic and responsive to short-term environmental shifts. Using a mesocosm design, we manipulated the duration of hydrologic conditions (i.e., stable dry, stable flooding, and alternating wet/dry) and the presence of plants to induce soil redox changes in wetland soils. We measured soil redox status, used targeted amplicon and shotgun metagenomic sequencing to characterize microbial communities, and measured greenhouse gas production to assess microbial function. The eight-week hydrologic treatment shifted community composition but did not override the stronger effects of long-term hydrologic history. Methane and carbon dioxide fluxes were altered by short-term hydrologic treatment, with methane production favored in the wet treatment and carbon dioxide production favored in the dry treatment. Plant presence versus absence manipulation had little impact on soil microbiome composition or soil greenhouse gas production. The results highlight the resistance of microbial community structure shaped by historical hydrologic regimes, and emphasize that hydrologic conditions exert a stronger influence than plant presence on microbial composition and function. Predicting the outcomes of wetland disturbance and restoration requires an enhanced understanding of community stability and functional plasticity. Our results suggest that wetland hydrologic restoration can establish a stable microbial community that is

resistant to environmental shifts, but microbial functions such as greenhouse gas emissions remain responsive to hydrologic disturbances, including flooding and drought.

Introduction

Wetlands, despite comprising only 5-10% of terrestrial land (Kingsford et al. 2016), have experienced at least a 21% loss globally (Fluet-Chouinard et al. 2023). These ecosystems are vital for water quality improvement and climate change mitigation through carbon sequestration (Mitsch et al. 2015). The conversion of wetlands for urban and agricultural development leads to the loss of these essential functions (Zedler and Kercher 2005). Consequently, there is significant interest in their conservation, restoration, and construction to leverage their ecosystem benefits (Spieles 2022; Patel et al. 2021; Suhani et al. 2020). Key wetland functions include anaerobic microbial processes in saturated soils, which facilitate complete inorganic nitrogen removal via denitrification and suppress aerobic organic matter decomposition (Mcleod et al. 2011; Martínez-Espinosa et al. 2021). However, these anoxic conditions can also support methanogenesis, potentially decreasing long-term carbon storage and climate benefits (Bridgham et al. 2013). The microbial functions delivering these ecosystem services are amenable to management for enhanced wetland benefits, necessitating a deeper understanding of the controls on wetland microbial ecosystem functions (Peralta, Stuart, et al. 2014). This gap in understanding microbial controls on ecosystem functions contributes to the limited success of current wetland restoration efforts, highlighting the need for further research (Cadier et al. 2020).

To produce cellular energy, microorganisms catalyze a series of oxidation-reduction (redox) reactions (Barron 1939; Walz 1979; Seto et al. 2025). Aerobic respiration yields the greatest amount of energy and is expected under dry conditions, but as water fills soil pore spaces, diffusion of oxygen (O_2) into the soil matrix decreases, causing a shift to a reducing environment (Truu et al. 2009; Mitsch et al. 2013; Marschner 2021). Reducing environments favor anaerobic respiration using terminal electron acceptors such as nitrate (NO_3^-), manganese, ferric iron, sulfate, and carbon dioxide (CO_2) (Burgin et al. 2011; Marschner 2021). Therefore,

measuring soil redox potential is useful for predicting which biogeochemical processes are likely to be carried out by soil microbes.

To manage microbial functions that support nitrogen removal and retention while reducing methane (CH_4) production, it is important to understand how changes in hydrology influence microbial communities. Microbial taxa are adapted to specific hydrologic conditions in their environment, and temporal changes in soil moisture (Peralta, Ludmer, et al. 2014; Truu et al. 2009; de Nijs et al. 2019; Ricks and Yannarell 2023). Drought, drainage, and soil re-wetting shift soil redox potentials, microbial community composition, and metabolism, which can influence the relative rates of anaerobic processes such as denitrification and methanogenesis (Kim et al. 2008; Truu et al. 2009; Peralta, Ludmer, et al. 2014; Fairbairn et al. 2023).

If drying and re-wetting events are periodic, a cycle of activity and dormancy can maintain higher microbial diversity than stable environmental conditions (Peralta, Ludmer, et al. 2014). For example, many denitrifiers are facultative anaerobes, capable of rapidly switching between aerobic respiration and denitrification (Tiedje et al. 1984; Sun et al. 2019; Freddi et al. 2023). Methanogens are often dominant in prolonged anoxic conditions, such as flooded wetlands, and are responsible for converting CO_2 or methyl groups to CH_4 (Mitsch and Gosslink 2007; Hernández et al. 2017; Ferry 2011). As hydrologic changes occur, oxic-anoxic interfaces support methanotrophs, which transform CH_4 to CO_2, and denitrifiers (McDonald and Murrell 1997; Mitsch and Gosslink 2007; Conrad 2009). This dynamic interplay between microbial guilds under fluctuating hydrologic conditions is therefore crucial for key transformations in carbon and nitrogen cycles.

While hydrology is a primary determinant of soil redox potential, plants also modify the soil environment. The soil microenvironments in contact with plant roots are hotspots of

microbial activity due to plant-mediated transport of nutrients, O_2, and carbon belowground (Kuzyakov 2010; Philippot et al. 2013; Chanton 2005). Additionally, vegetation can alter soil redox potentials by facilitating transport of O_2 into root zones (Chanton 2005; Sundberg et al. 2007) and transporting CH_4 from root zones into the atmosphere (Carmichael et al. 2014; Hu et al. 2015).

Climate change is projected to increase the frequency of both flooding and drought in the southeastern US, while ongoing land use change continues to reduce wetland and forest cover (Apurv and Cai 2021; IPCC 2023; Easterling et al. 2017; Skeeter et al. 2019; Terando et al. 2014; Griffith et al. 2003; Potapov et al. 2022). These large-scale shifts in hydrology and vegetation represent a major disturbance to wetland soil microbiomes. Understanding and predicting the functional responses of these microbiomes is difficult because their stability is based on a complex network of biotic and abiotic interactions (Griffiths and Philippot 2013; Lennon et al. 2023; Treseder et al. 2012).

Microbial stability is defined by two key properties: resistance (insensitivity to disturbance) and resilience (the rate of recovery post-disturbance) (Shade et al. 2012; Pimm 1984). Following a disturbance, a shift in community function can be driven by two different mechanisms: compositional change (a shift in who is there) or phenotypic plasticity (a change in what the existing microbes are doing) (König et al. 2018; Philippot et al. 2021). Soil microbiome stability is also influenced by abiotic factors, including soil texture, substrate diversity, and nutrient availability (Griffiths and Philippot 2013). Functional and taxonomic characterization of microbiome responses to hydrologic and plant disturbance can help refine predictions of wetland greenhouse gas (GHG) emissions.

This study investigated the effects of hydrologic change duration (i.e., sustained dry, interim dry/wet, sustained wet) and vegetation presence on microbial community structure, soil redox conditions, and GHG production. We hypothesize that hydrologic history will have a greater impact on microbial community composition than eight weeks of hydrologic and plant presence/absence treatments. While we expect community composition to be resistant to change over eight weeks of incubation, we also hypothesize that short-term hydrologic and plant presence/absence treatments will impact GHG production through community phenotypic plasticity combined with a more limited shift in community composition. Predicted functional responses include increased methanogenesis in reducing conditions (wet and no plants) and increased aerobic respiration in oxidizing conditions (dry and plants).

To test these hypotheses, we conducted a mesocosm experiment in which we manipulated hydrology (i.e., dry, interim, and wet) and the presence of plants in soils collected from different hydrologic histories (i.e., dry, wet/dry transition, and saturated wet zones) within a restored coastal plain wetland. We measured soil nutrient concentrations, redox potentials, GHG fluxes, and characterized soil microbial communities using shotgun metagenomic and 16S rRNA gene amplicon sequencing. By imposing acute differences in hydrology and plant cover, we were able to test plant-microbe responses to long-term hydrological regimes versus short-term hydrological disturbances, and the associated net ecosystem greenhouse gas outputs.

Methods

Study site

We collected soil samples from the Timberlake Observatory for Wetland Restoration (TOWeR) located in the Albemarle Peninsula in Tyrell County, North Carolina (35°54’22” N

142 76°09’25” W; Figure 1). The site is part of the Great Dismal Swamp Restoration Bank, which is
143 a 1,700 ha wetland consisting of 420 ha of mature forested wetland, 787 ha of forested wetland,
144 57.2 ha of drained shrub-scrub, and 440 ha of agricultural fields restored to wetland habitat in
145 2007 (Ardón et al. 2010; 2013; Morse et al. 2012). A major portion of the restoration effort was
146 to remove drainage ditches and plant 750,000 saplings, including *Taxodium distichum, Nyssa*
147 spp., *Salix nigra, Fraxinus pennsylvanica*, and *Quercus* spp. (Morse et al. 2012). A more recent
148 survey indicates that the dominant plant species at the site is *Juncus effusus* L., along with
149 *Euthamia caroliniana* (L.) Greene ex Porter & Britton, *Solidago fistulosa* Mill., and *Scirpus*
150 *cyperinus* (L.) Kunth (Hopfensperger et al. 2014). The site is connected to the Albemarle Sound
151 via the Little Alligator River, and the site’s position in the landscape increases the potential for
152 saltwater intrusion to occur (Ardón et al. 2013). Even though there is little elevation change (-1
153 m to 2 m) across the restored wetland, there is a hydrologic gradient, which is driven by the
154 position of the water table and represents upland dry, saturated wet, and transition dry/wet
155 (“interim”) sites (Hopfensperger et al. 2014).
156
157 *Mesocosm experimental design*
158 We used a mesocosm approach to assess the changes in the soil microbial community,
159 redox potentials, and GHG production due to hydrologic changes and vegetation. We set up a
160 mesocosm experiment using soil blocks collected from three sites within the TOWeR. Soils were
161 collected from the restored portion of the site (12 years post-restoration), which had been used as
162 agricultural fields for several decades before restoration (Ardón et al. 2010). We collected soils
163 that represented three different hydrologic zones on the inflow side of the site at the following
164 coordinates: 35.895917° N 76.165972° W (dry), 35.895778° N 76.165861° W (interim), and

35.895639° N 76.165556° W (wet). Six intact soil blocks (25 cm × 25 cm × 20 cm deep) were cut out from each of the three sites using landscaping knives and shovels. Soil hydrologic history was determined by water table levels at the time of collection (dry = 20 cm, interim = 10 cm, and wet = 0 cm below surface level). Soil blocks were contained in dark plastic containers of the same dimensions as the soil blocks (Figure 1).

To manipulate the presence of vegetation, the container was divided in half and separated by a root screen (20 µm stainless steel mesh). On one side, plants were allowed to grow during the experiment, while the 'no plant' side was maintained by careful removal of above- and belowground plant biomass. To manipulate hydrology within the mesocosm, vinyl tubing was inserted 3 cm from the bottom of the mesocosm container on each side and connected to a 1 L water bottle (Figure 1). Water levels inside the mesocosm were maintained by filling the 1 L bottle to the desired height using rainwater collected from a cistern. Finally, 10 cm diameter schedule 40 polyvinyl chloride (PVC) collars were inserted 5 cm below the surface as a sampling base for GHG chambers (described in subsection *GHG fluxes*). The mesocosm experiment was housed at East Carolina University (ECU) West Research Campus (Greenville, NC) under a covered hoop house with a shade cloth, which prevented precipitation and allowed 60% light penetration. Soils were collected on April 1, 2016, and prepared on May 29, 2016. Experimental mesocosm sampling commenced on June 13, 2016, and concluded on August 11, 2016. Temperatures ranged from 22.7 °C to 30.8 °C during the experiment. Because the hoop house was in a wetland approximately 150 km from the field site, within the same physiographic region, the temperature and relative humidity in the hoop house would have closely resembled field conditions. Blocking precipitation was essential for the controlled manipulation of hydrologic conditions.

188 Two weeks after installing PVC collars and setting up the plant treatment, we started
189 hydrologic treatments. Hydrologic manipulation occurred over eight weeks to allow for multiple
190 dry/wet transitions for the interim treatment. Mesocosms exposed to wet conditions were flooded
191 by overhead watering and maintained using water reservoirs filled to maximum container height
192 (18 cm). Mesocosms exposed to dry conditions were maintained using water reservoirs filled to a
193 depth of 5 cm. The dry/wet (interim) treatments fluctuated between flooded and dry conditions,
194 as described above, every two weeks, starting with a wet treatment and ending with a dry
195 treatment.
196 All mesocosm plants originated from the standing plant community and seed bank
197 (described in Hopfensperger et al. 2014). We did not monitor plant community composition, but
198 we did observe general differences in mesocosm plant communities based on hydrologic
199 treatment. Continuously flooded mesocosms were often dominated by aquatic and semi-aquatic
200 plants like *Ludwigia palustris*, while interim and dry mesocosms contained a higher proportion
201 of sedges and *J. effusus*.
202
203 *Measuring integrated soil redox status*
204 We measured soil redox status at the beginning and end of the experiment using Indicator
205 of Reduction in Soils (IRIS) tubes (InMass Technologies, Figure 2, Appendix S1: Figure S1).
206 The IRIS tubes are constructed from 1.5 cm diameter schedule 40 PVC pipe coated in iron oxide
207 (Fe(III)) paint (Rabenhorst 2008). In oxidizing conditions, Fe(III) appears as an orange-red paint;
208 but when exposed to reducing conditions, Fe(III) is reduced to Fe(II), which dissolves in
209 solution, leaving a white clearing on the tube (Jenkinson and Franzmeier 2006; Rabenhorst
210 2008). At the beginning of the experiment, two IRIS tubes (12 cm depth) were installed in each

mesocosm: one on the plant side and one on the bare soil side. The IRIS tubes were incubated in mesocosms for two weeks before removal and analysis. After we removed the IRIS tube, a non-coated PVC pipe was used to fill the hole. Two weeks before the end of the experiment, the non-coated PVC pipe was removed and replaced with a new IRIS tube to measure soil redox status at the end of the experiment.

We quantified the surface area of Fe(III) paint removed from IRIS tubes. First, we imaged the entire tube by taking four pictures and then stitched the photos into a composite using *GIMP2* (v2.8.14) (Kimball et al. 2014). Next, we identified areas of artificial paint removal (i.e., scratches from installing or removing tubes) and manually filled these pixels. Then, using *ImageJ* (v1.48) (Schneider et al. 2012), we converted all colored pixels to black. We compared the number of white pixels to the total pixels to determine the percentage of paint removed. Interpretation of redox status is based on the percent paint removed from a 10 cm section of tubing and summarized as follows: 0% not reducing, 1-5% probably not reducing, 5-10% possibly reducing, 10-25% and >25% definitely reducing (Rabenhorst 2008). For regression analyses, the percent of paint removed was treated as a continuous variable.

Soil physicochemical characteristics

Soil properties were determined from soils collected during the destructive sampling of mesocosms at the end of the experiment. We collected six soil cores (3 cm diameter, 10 cm depth) from each side of the box (i.e., plant and no plant) and combined cores collected from one side into a composite sample (i.e., one plant composite and one no plant composite), passed soils through a 4 mm sieve, and homogenized samples before subsampling for soil analyses. For each sample, we measured gravimetric soil moisture by drying 20-30 g of field-moist soil at 105 °C

234 for at least 24 hours. Approximately 5 g of field-moist soil was extracted with 45 ml of 2 M KCl,
235 and extractable ammonium (NH_4^+) and NO_3^- ions were colorimetrically measured using a
236 SmartChem 200 auto analyzer (Unity Scientific, Milford, Massachusetts, USA) at the ECU
237 Environmental Research Laboratory. To determine total carbon and total nitrogen (TC, TN), a
238 subsample of air-dried soil was finely ground and sieved through a 500 µm mesh and analyzed
239 using an elemental analyzer (2400 CHNS Analyzer; Perkin Elmer, Waltham, Massachusetts,
240 USA) at the Environmental and Agricultural Testing Service Laboratory, Department of Crop
241 and Soil Sciences, North Carolina State University. A second subsample of air-dried soil was
242 sent to Waters Agricultural Laboratories, Inc. (Warsaw, NC) and analyzed for pH, phosphorus,
243 potassium, magnesium, sulfur, manganese, iron, and humic matter, using standard Mehlich III
244 methods (Mehlich 1984; Mylavarapu et al. 2014).
245
246 *Greenhouse gas (GHG) fluxes*
247 We examined the effects of hydrology and vegetation on GHG production. We measured
248 GHG fluxes on June 13, 2016, two weeks after hydrologic treatments were established, and then
249 every two weeks until August 11, 2016, for a total of five sampling events. The GHG collection
250 chambers were 20 cm in height with a diameter of 8.25 cm and constructed from clear acrylic
251 tubing. GHG fluxes were measured using transparent chambers, thus representing net fluxes of
252 heterotrophic and autotrophic plant and microbial activity. Chambers were sealed on one end
253 with silicon and a pipe cap with a 33 mm septum installed as a gas sampling port. At the time of
254 sampling, chambers were placed on top of preinstalled PVC collars, and the seals were taped to
255 prevent diffusion from the seam (Hoffmann et al. 2018). A gas sample was collected from the
256 chambers at four time points: 30, 60, 120, and 180 minutes after the chambers were attached.

Initial ambient (T_0) samples were not obtained before chamber closure. Instead, they were collected from the mesocosm incubation field site at the ECU West Research Campus as part of a 16-month effort to sample coastal plain wetland GHGs, spanning from August 2021 to December 2022. Monthly average ambient GHG concentrations were calculated and used to represent the T_0 concentration for mesocosm flux measurements within each corresponding month. To collect gas samples, we used a needle attached to a 20 mL syringe, mixed headspace gas three times by pulling and depressing the plunger, and then collected a 20 mL sample. Gas samples were equally distributed between two 3 mL glass Exetainer vials (Lampeter, Wales, UK) fitted with screw top and dual-layer septa. Samples were stored upside down at room temperature in a dark location and were analyzed within 96 hours of collection.

We analyzed GHG concentrations using a Shimadzu gas chromatograph (GC-2014) fitted with an electron capture detector to detect N_2O and a flame ionization detector with a methanizer to measure CH_4 and CO_2. Calibration standards are listed in Appendix S1: Table S1. If a sample measured above the calibration curve, we diluted the sample, remeasured the concentration, and accounted for the dilution factor when calculating the final concentrations. After the first two time points, calibration curves were adjusted to accommodate larger GHG concentrations (Appendix S1: Table S1). Since all unknown concentrations were analyzed within the bounds of their calibration curve, results were unaffected by adjustments to the calibration curves.

We calculated GHG fluxes using the *gasfluxes* package implemented in the R Statistical Environment and RStudio (RStudio 2024.12.0+467, Rv4.4.2) (Fuss and Hueppi 2024; R Core Team 2024). The best model fit among HMR, robust linear, and linear was selected for each flux (Appendix S2).

280 *Bacterial and archaeal community analyses*

281 We assessed the soil microbial community composition at the beginning ('start', based on
282 soils collected from the IRIS tube installation) and end of the experiment ('final', based on soils
283 collected during destructive sampling). We collected 'final' soil samples using a standard soil
284 probe (3 cm diameter, 10 cm depth) from the same location that we collected GHG samples. We
285 extracted genomic DNA from the soils using the Qiagen DNeasy PowerSoil Kit and diluted the
286 DNA to 20 ng/µL. This genomic DNA was used as template in PCR reactions with barcoded
287 primers (bacterial/archaeal 515FB/806R primer set) originally developed by the Earth
288 Microbiome Project to target the V4 region of the bacterial 16S subunit of the ribosomal RNA
289 gene (Caporaso et al. 2012; Apprill et al. 2015; Parada et al. 2016). PCR reactions and
290 sequencing library preparation are described in Appendix S1: Supplemental Methods. We
291 sequenced the pooled libraries using the Illumina MiSeq platform using paired-end reads
292 (Illumina Reagent Kit v2, 500 reaction kit) at the Indiana University Center for Genomics and
293 Bioinformatics Sequencing Facility.

294 Sequences were processed using the *mothur* (v1.42.0) MiSeq pipeline (Kozich et al.
295 2013; Schloss et al. 2009). We assembled contigs from the paired-end reads, quality trimmed
296 using a moving average quality score (minimum quality score 35), aligned sequences to the
297 SILVA rRNA database (v132) (Quast et al. 2013), and removed chimeric sequences using the
298 VSEARCH algorithm (Rognes et al. 2016). We created operational taxonomic units (OTUs) by
299 first splitting sequences based on taxonomic class and then binning them into OTUs based on
300 97% sequence similarity. Since amplicon sequencing was conducted using short reads (250 bp)
301 and not assembled genomes, we used an OTU-based 3% distance threshold to avoid splitting the
302 same bacterial genome into distinct clusters (using amplicon sequence variant (ASV) of a single

303 base difference). An OTU-based approach also limits over-inflated numbers of ASVs introduced
304 by PCR bias and sequencing errors (Schloss 2021). In addition, employing an OTU- or ASV-
305 based approach is known to result in similar broadscale community composition patterns
306 (Glassman and Martiny 2018).
307
308 *Shotgun metagenomic analyses*
309 Based on amplicon sequencing, we identified a subset of samples representing the most
310 distinct microbial communities for shotgun metagenomic sequencing. A description of sample
311 processing and metagenomic sequencing can be found in Peralta et al. (2020). Briefly, we chose
312 a set of baseline and post-flooding/drying treatment samples. We sourced mesocosm baseline
313 conditions from relatively dry (water level at about -20 cm, n = 4) and relatively wet (water level
314 at about 0 cm, n = 4) field locations. At the end of the eight-week experiment, we selected a
315 subset of samples from the hydrologic treatments (prolonged drying or wetting only) and plant
316 treatments (presence or absence of vegetation) (n = 16). After genomic DNA extraction using the
317 Qiagen DNeasy PowerMax soil kit, samples were sent to the U.S. Department of Energy (DOE)
318 Joint Genome Institute (JGI) for sequencing and analysis (GOLD study ID Gs0142547 and
319 NCBI BioProject accession number PRJNA641216). Plate-based DNA library preparation and
320 subsequent Illumina sequencing, according to published protocols (Peralta et al. 2020), resulted
321 in 583.2 Gbp of raw sequence data. Raw data were processed using the DOE JGI Metagenome
322 Annotation Pipeline IMG/M v.5.0.9 (Chen et al. 2017; Huntemann et al. 2016; Markowitz et al.
323 2014).
324 From the metagenomes, we curated functional gene sets using IMG/M's integrated Kyoto
325 Encyclopedia of Genes and Genomes (KEGG) module list. For statistical analyses, we focused

326 on the following four functional gene sets associated with biogenic greenhouse gas fluxes: (1)
327 Denitrification (KEGG Module M00529), (2) Methanogen (M00617), (3) Central Carbohydrate
328 Metabolism (M00001-M00011, M00307-M00309, M00580, and M00633), and (4) Prokaryotic
329 Cytochrome C Oxidase (CcO) (M00155).
330
331 *Statistical Analyses*
332 All statistical analyses were performed in the R statistical environment (RStudio
333 2024.12.0+467, Rv4.4.2) (R Core Team 2024). Before multivariate statistical analyses, we
334 normalized sample-to-sample variation in sequence depth by taking the relative abundance of
335 each OTU. OTU data were then rarefied using *vegan::rrarefy* (Oksanen 2015). Likewise,
336 functional gene counts were converted to relative abundance by dividing the count of each
337 functional gene by the total number of functional gene counts in each respective functional gene
338 category. We examined beta diversity by visualizing bacterial community responses to
339 hydrologic history (field conditions), hydrologic treatment (contemporary dry/wet treatments),
340 and plant presence/absence using principal coordinates analysis (PCoA) of bacterial community
341 composition based on Bray-Curtis dissimilarity. We also used PCoA to visualize the Bray-Curtis
342 dissimilarity of functional gene categories according to hydrologic history, hydrologic treatment,
343 and plant presence/absence. We used permutational multivariate analysis of variance
344 (PERMANOVA) to determine differences between bacterial communities among hydrologic
345 history, hydrologic treatment, and plant presence. Hypothesis testing using PERMANOVA was
346 performed using the *vegan::adonis* function (Oksanen 2015). Unique taxa representing each
347 hydrologic history and hydrologic treatment were determined by Dufrene-Legendre indicator
348 species analysis using the *labdsv::indval* function (Roberts 2023). Finally, soil properties were

compared against bacterial community and functional patterns (based on Bray-Curtis dissimilarity) using the *vegan::envfit* function (Oksanen 2015). Soil properties with $p \leq 0.05$ were represented on the PCoA plot of 16S rRNA community composition as vectors scaled by their correlation to microbial community patterns. The GHG fluxes and soil properties with $p \leq 0.1$ were plotted as vectors, scaled by their correlation, on PCoA plots of functional gene composition.

We constructed linear mixed effects models with sampling plot (mesocosm) and sampling date as random effects to determine the importance of the fixed effects of hydrologic history (field conditions), hydrologic treatment (contemporary dry/wet treatments), and plant presence on GHG fluxes using the *lme4* R package (Bates et al. 2015). Then, we used Akaike's Information Corrected Criterion (AICc) model comparisons to determine the simplest combination of fixed effects needed to explain the most variance in GHG fluxes (Hurvich and Tsai 1993; Gorsky et al. 2019). We did not use the interaction between the fixed effects hydrologic history and hydrologic treatment because combinations would have resulted in a sample size of $n = 2$ for each group. Lastly, to determine the proportion of variance explained by fixed effects (marginal) and the complete model (conditional), we used the *MuMIn* R package (Gorsky et al. 2019; Bartoń 2025).

While linear mixed effects models are robust to departures from normality (Schielzeth et al. 2020), traditional ANOVAs and t-tests are less so (Blanca et al. 2017; Havlicek and Peterson 1974). To accommodate extreme outliers and lack of normality, we used nonparametric statistics to test for differences in GHG fluxes among hydrologic treatments and plant presence/absence. We used Wilcoxon Rank Sum tests to assess differences in GHG fluxes between plant and no plant groups, and Kruskal-Wallis tests to compare GHG fluxes among the three hydrologic

372 treatments (dry, interim, and wet). To account for repeated measures, the Wilcoxon Rank Sum
373 and Kruskal-Wallis tests were grouped by sampling date. If the Kruskal-Wallis test for a
374 sampling date revealed differences among treatment groups ($p \leq 0.05$), we then performed
375 pairwise comparisons using the Dwass, Steel, Critchlow, and Fligner (SDCFlig) test with a
376 Monte Carlo distribution (Schneider et al. 2023).

377 To assess microbial community structure and function relationships, we examined the
378 relationship between GHG fluxes and microbial community/functional Bray-Curtis dissimilarity
379 matrices using distance-based partial least squares regression (DBPLSR) in the *dbstats* R
380 package (Boj et al. 2024). Finally, we used the *vegan::mantel* function (Oksanen 2015) to
381 examine the relationship between the soil properties (redox, percent moisture, pH, NH_4^+, total
382 soil C, total soil N, phosphorus ppm, potassium ppm, magnesium ppm, sulfur ppm, iron ppm,
383 manganese ppm, and percent humic matter), GHG fluxes, and microbial community
384 composition.

385

386 **Data Availability**

387 All code and data used in this study are in a public GitHub repository
388 (https://github.com/PeraltaLab/WetlandMesocosm_GHG_Timberlake) with a Zenodo DOI
389 (https://doi.org/10.5281/zenodo.15528281). Raw amplicon sequence files can be found at NCBI
390 SRA BioProject ID PRJNA636184, and metagenome sequence files can be found at NCBI
391 SRA BioProject ID PRJNA641216.

392

393 **Results**

394 Soil mesocosms sampled from three distinct hydrologic conditions (dry, interim, wet),
395 were subjected to eight weeks of hydrologic and plant presence/absence treatments (Figure 1).
396 The three levels of hydrologic treatments were: (1) flooded for eight weeks, (2) dry for eight
397 weeks, and (3) interim, i.e., two weeks flooded alternating with two weeks dry for a total of eight
398 weeks. Each box was separated by a stainless mesh divider, with plants allowed to grow on one
399 side and plants removed on the other side (Figure 1).
400
401 *Characterization of soil physical-chemical properties*
402 There was little variability in soil properties across main effects (hydrologic history,
403 hydrologic treatment, plant presence), except for notable differences in soil moisture between
404 plant treatments within dry and wet hydrologic treatments (Table 1). In addition, NO_3^-N
405 concentrations were below the detection limits in samples with plants, but measurable in samples
406 without plants (Table 1). Soil redox status as measured by IRIS tubes revealed that soils
407 experiencing dry and interim treatments were not reducing (0% iron oxide paint removed), while
408 soils in wet treatments were reducing (Figure 2). In wet treatments, localized oxidizing
409 conditions were maintained on portions of IRIS tubes in contact with roots (Figure 2, Appendix
410 S1: Figure S1).
411
412 *Plant and soil redox effects on greenhouse gas fluxes*
413 *Methane (CH_4)*
414 Wet hydrologic treatment and no plants produced the highest CH_4 fluxes and the greatest
415 variability between samples (10.31 ± 45.54 mg CH_4 m^{-2} h^{-1}, $\bar{x} \pm SD$, Appendix S1: Table S2).
416 When comparing plant vs. no plant CH_4 fluxes at each of the five time points, no differences

were detected, except during the second time point on June 28th, where CH_4 concentrations were greater in the presence of plants than in the absence of plants (Appendix S1: Figure S2, Table S3). The wet treatment produced greater CH_4 fluxes than the dry treatment throughout the middle three time points (June 28th through July 25th), and differences in wet vs. interim and dry vs. interim were observed but did not persist throughout the experiment (Figure 3, Appendix S1: Table S4). The linear mixed-effects model with random effects only (sample mesocosm and date) was the most plausible (ΔAICc = 0), with an AICc weight of 0.37 (Appendix S1: Table S5).

Carbon dioxide (CO_2)

CO_2 fluxes in the dry hydrologic treatment were greater than CO_2 fluxes in the interim and wet treatments during two out of five time points (Figure 3, Appendix S1: Table S4). The linear mixed effects model, which included the interactive effects of hydrologic treatment and plant presence/absence, was the most plausible (ΔAICc = 0), and explained 49% of the variance in CO_2 fluxes (conditional R^2, Appendix S1: Table S5). In comparison, the fixed effect of plant presence/absence explained 12% of the variance in CO_2 fluxes, and hydrologic treatment and hydrologic history explained 19% and 1%, respectively (Appendix S1: Table S5).

Nitrous oxide (N_2O)

The N_2O fluxes were near zero in all hydrologic and plant treatments (range: -4.61 – 2.88 mg N_2O m^{-2} h^{-1}) (Figure 3, Appendix S1: Figure S2). On July 11th and July 25th, no plant N_2O fluxes exceeded plant N_2O fluxes (Appendix S1: Figure S2, Table S3). The N_2O fluxes were similar among hydrologic treatments, except for lower fluxes in interim hydrology on June 13th

(Figure 3, Appendix S1: Table S4). The model with plant and hydrologic treatment additive effects was most plausible (ΔAICc = 0), based on an AICc weight of 0.25 (Appendix S1: Table S5).

Relationship between soil redox conditions and GHG fluxes

We used linear regression to examine the relationship between soil redox status (represented by the percent of paint removed from IRIS tubes) and GHG fluxes. At the start of the experiment, the CH_4 fluxes had a weak positive relationship with redox status ($F_{34} = 3.14$, $R^2 = 0.06$, $p = 0.09$, Appendix S1: Table S6, Figure S3). At the end of the experiment, the CO_2 fluxes had a negative relationship with redox conditions ($F_{34} = 6.90$, $R^2 = 0.14$, $p = 0.01$, Appendix S1: Table S6, Figure S3). The N_2O fluxes were not significantly related to redox conditions throughout the experiment (Appendix S1: Table S6, Figure S3).

Patterns in microbial community composition

Bacterial and archaeal community composition clustered by hydrologic treatment within hydrologic history (Figure 4). Hydrologic history (PERMANOVA, $F_{2, 35} = 7.562$, $R^2 = 0.305$, $p = 0.001$) and hydrologic treatment (PERMANOVA, $F_{2, 35} = 2.605$, $R^2 = 0.110$, $p = 0.002$) explained variance in microbial community patterns (Figure 4, Appendix S1: Table S7). In contrast, microbial community composition was similar in the presence or absence of plant communities (PERMANOVA, $F_{1, 35} = 0.698$, $R^2 = 0.102$, $p = 0.824$, Appendix S1: Table S7). Overall patterns in microbial composition and soil properties were significantly correlated (Mantel $r = 0.384$, $p = 1.0 \times 10^{-4}$, Appendix S1: Table S8).

462 Indicator species analysis of the top 2.5% of OTUs (by relative abundance at a
463 significance level of $p \leq 0.01$) revealed that dry history was represented by aerobic bacterial
464 genera (*Gaiella*, *Reyranella*, and *Terrimonas*). Microbial taxa putatively associated with methane
465 cycling, including the archaeal genus *Methanobacterium* and the bacterial genera *Methylocystis*
466 and *Syntrophobacter,* were unique to microbial communities from wet hydrologic histories
467 (Appendix S1: Table S9). Wet treatment was indicated by nitrogen-fixing taxa,
468 *Anaeromyxobacter* and *Bradyrhizobium*, while *Reyranella* signaled both dry historical conditions
469 and wet hydrologic treatment (Appendix S1: Table S10).
470
471 *Patterns in functional gene composition*
472 The composition of functional genes was influenced by hydrologic conditions, but not by
473 the presence or absence of plants. Carbohydrate metabolic composition differed between
474 hydrologic treatments (PERMANOVA, $F_{1, 23} = 2.735$, $R^2 = 0.092$, $p = 0.013$), while
475 denitrification, methanogenesis, and CcO genes were similar across hydrologic treatments
476 (Appendix S1: Table S7). Hydrologic history influenced the composition of genes associated
477 with methanogenesis, central carbohydrate metabolism, and CcO (Appendix S1: Table S7).
478 Based on environmental fitting (*vegan::envfit*), denitrification functional gene
479 composition correlated with carbon losses via CO_2 flux (envfit, $R^2 = 0.243$, $p = 0.063$, Figure 5).
480 The PCoA of methanogenesis genes correlated with percent soil moisture (envfit, $R^2 = 0.201$, $p =$
481 0.094), and the PCoA of central carbohydrate metabolism genes correlated with the percent of
482 paint removed from IRIS tubes (envfit, $R^2 = 0.238$, $p = 0.059$, Figure 5). The composition of
483 CcO genes did not vary significantly with either GHG fluxes or soil redox conditions (Figure 5).
484

Relationships between GHG fluxes, microbial community composition, and soil properties

Microbial community composition explained more variance in GHG fluxes than did soil properties. DBPLSR revealed that microbial community composition explained 58%, 37%, and 47% (components 1 and 2) of the variance in concentrations of CH_4, CO_2, and N_2O fluxes, respectively (Appendix S1: Table S11). Patterns in soil properties, on the other hand, only explained 19%, 29%, and 26% of the variance in concentrations of CH_4, CO_2, and N_2O fluxes, respectively, based on components 1 and 2 (Appendix S1: Table S11).

We evaluated relationships among the variance in GHG fluxes and functional gene composition at the beginning and end of the experiment using DBPLSR. Denitrification gene composition explained 54% of the variance in N_2O production at the start of the experiment, and 60% of the variance in N_2O fluxes at the end of the experiment (Appendix S1: Table S11, components 1 and 2). Methanogenesis functional gene composition explained a higher proportion of variance in CH_4 fluxes in 'start' samples (63%) than 'final' samples (33%) (Appendix S1: Table S11, components 1 and 2). 'Start' compositions of CcO and carbohydrate metabolism explained 91% and 98% of variance in CO_2 fluxes, respectively (Appendix S1: Table S11, components 1 and 2). At the end of the experiment, CcO composition only accounted for -0.007% of the variance in CO_2 fluxes, while carbohydrate metabolism explained 40% of the variance in CO_2 fluxes (Appendix S1: Table S11, components 1 and 2).

Discussion

This study revealed that historical hydrologic conditions influenced microbial taxonomic and functional composition more strongly than eight weeks of hydrologic treatments and plant removal manipulation. Hydrologic treatments impacted CH_4 and CO_2 fluxes but had little effect

508 on N_2O fluxes. Plant presence mitigated flood-induced reducing conditions in the rhizosphere
509 but did not shift microbial community composition or soil GHG fluxes. These findings highlight
510 the resistance of soil microbial community composition to short-term changes in hydrology and
511 plant cover, indicating that a more plastic shift in community function underlies responses in
512 CH_4 and CO_2 fluxes to hydrologic treatments.
513
514 *Past hydrology dictates bacterial community composition*
515 Hydrologic history was a stronger driver of microbial community composition than our
516 eight-week manipulation of hydrology and plant presence (Figure 4, Appendix S1: Table S7),
517 indicating strong community resistance. This resistance was likely established through a
518 combination of priority effects and protected soil microenvironments. During soil colonization
519 following wetland restoration, priority effects would have allowed early arriving microbes to
520 occupy the most favorable niches within the newly established hydrologic and vegetation
521 regimes (Fukami et al. 2010; van de Voorde et al. 2011). Over time, this process leads to
522 resource partitioning where organisms fill available niches and prevent the establishment of
523 incoming taxa (Northfield et al. 2010). Additionally, hydrologic and plant manipulations may not
524 have sufficiently altered the soil microenvironments (e.g., soil aggregates), which could have
525 buffered the microbial community against environmental disturbance (Zhao et al. 2024; Ran et
526 al. 2020). Soil physicochemical properties and microbial community composition are
527 intertwined, and therefore, the relative impacts of biotic vs. abiotic controls on microbiome
528 stability are difficult to distinguish (Griffiths et al. 2008; Griffiths and Philippot 2013).
529 Collectively, the assembly and establishment by a historically adapted community and the
530 persistence of soil microenvironments would maintain compositional stability, explaining why

the short-term press disturbance from our treatments did not overpower the legacy community composition.

Our indicator species analysis provides evidence for observed legacy effects. For instance, the strictly aerobic genus *Gaiella* was an indicator for soils with a dry history (Albuquerque et al. 2011). In contrast, taxa associated with anaerobic processes like methanogenesis and iron reduction were indicators of soils with a wet history (Appendix S1: Table S9). Further evidence for how soil history confers resistance comes from the genus *Reyranella*, which was a significant indicator for soils with a dry history and those subjected to wet treatment. *Reyranella* is an aerobic genus in the family *Rhodospirillaceae* with variable capacity for nitrate reduction (Lee et al. 2017). This suggests *Reyranella* relied on aerobic respiration in the dry-history soils. When the mesocosms were flooded, *Reyranella* likely shifted from aerobic respiration to NO_3^- reduction, using this metabolic flexibility to increase in relative abundance. This is an example of the community absorbing the disturbance via taxa already equipped for that specific environmental change, thereby maintaining compositional stability. While hydrologic history was the strongest driver of community composition, hydrologic treatment created a smaller but significant separation in community composition (Figure 4, Appendix S1: Table S7). This shift in composition, combined with changes in community activity, may explain observed differences in CH_4 and CO_2 fluxes.

Dynamic hydrology influences greenhouse gas production more than plant presence versus absence

CH_4 fluxes were highest, and CO_2 fluxes were lowest in soils experiencing the wet hydrologic treatment (Figure 3). In the wet treatment, oxidizing conditions were maintained by

plant roots and resulted in an organic plant root pattern due to oxidized iron paint on the IRIS tubes (Figure 2, Appendix S1: Figure S1). We expected that O_2 radiation from plant roots would decrease soil CH_4 fluxes by providing methanotrophs with O_2 for CH_4 consumption and supporting aerobic respiration at the expense of obligate anaerobic metabolisms like methanogenesis. However, methanotrophic functional gene composition was unresponsive to the presence or absence of plants (Finlay and Peralta 2025), and random effects (sample mesocosm and date) predominantly explained CH_4 fluxes (Appendix S1: Table S5). Localized O_2 availability adjacent to roots was insufficient to shift the bulk soil community composition or net CH_4 fluxes. Patterns in net CH_4 flux are further complicated by aerobic and anaerobic methanotrophs distributed across soil O_2 gradients (e.g., hydrologic gradients) (Maietta et al. 2020). Despite the prevalence of random effects, the higher CH_4 fluxes observed in wet versus dry treatments align with extensive literature reporting greater CH_4 fluxes in saturated soils. (Christiansen et al. 2016; Maietta et al. 2020; Fairbairn et al. 2023). While CH_4 and N_2O fluxes were similar in the presence and absence of plants, CO_2 fluxes displayed a predictable decline in the presence of plants.

The observed decline in CO_2 fluxes in the presence of plants was unsurprising due to plant photosynthesis and fixation of atmospheric CO_2 from within the transparent collection chamber (Luan and Wu 2014). The elevated CO_2 fluxes in the dry hydrologic treatment are presumably due to aerobic respiration. A comparison of O_2 and soil moisture impacts on CO_2 fluxes found the greatest CO_2 fluxes in intermediate soil moisture (Fairbairn et al. 2023). Percent soil moisture was moderate in our dry treatment ($\bar{x}$ = 26.5%, Table 1). The moderate moisture likely promoted access to O_2 while maintaining sufficient water content for dissolved C substrate access (Fairbairn et al. 2023). Plants consistently decreased CO_2 fluxes throughout the

experiment, while differences in GHG fluxes between hydrologic treatments were more variable. Therefore, models of wetland GHG emissions should consider plant cover as a stable control of CO_2 fluxes. Conversely, the impacts of soil moisture on GHG fluxes vary dynamically over time and may require finer temporal resolution soil moisture measurements to model GHG fluxes accurately.

Functional gene composition predicts greenhouse gas fluxes to varying degrees

Cytochrome C oxidase

We analyzed the composition of prokaryotic CcO genes as an indicator of aerobic respiration in oxidizing conditions. While hydrologic history influenced CcO composition, CcO composition did not explain significant variance in GHG fluxes during the eight-week incubation (Figure 5, Appendix S1: Table S7, Table S11). This lack of explanatory power is unsurprising, given the diversity of O_2-reducing terminal oxidases and the known presence of CcO genes in strict anaerobes (Esposti 2020; Jabłońska and Tawfik 2019). There is no single enzyme that can be used to distinguish aerobic and anaerobic phenotypes because aerobic and anaerobic organisms do not exist as binary groups (Jabłońska and Tawfik 2019). Instead, a spectrum of oxygen usage phenotypes exists (Jabłońska and Tawfik 2019). Evaluating the presence and number of a full suite of O_2-utilizing enzymes may be a useful indicator of aerobic vs. anaerobic status (Jabłońska and Tawfik 2019). Therefore, bioinformatic methods to facilitate this method ought to be further developed.

Central carbohydrate metabolism

While CcO composition was unable to explain differences in CO_2 production across treatments, the composition of central carbohydrate metabolism genes was strongly related to differences in hydrologic history, hydrologic treatment, and the production of CO_2 (Figure 5, Appendix S1: Table S7, Table S11). A previous study found a significant positive correlation between the abundance of carbohydrate-active enzymes and cumulative respiration in a tundra soil warming experiment (Johnston et al. 2019). Similarly, carbohydrate metabolism genes predicted differences in soil respiration between paddy and upland soils (Liu et al. 2020). While there is no single gene or defined collection of genes that have been consistently used to explain microbial community respiration responses to redox changes, various collections of carbohydrate metabolism genes often reflect differences in soil redox status and respiration (Johnston et al. 2019; Liu et al. 2020).

Denitrification

The composition of denitrification functional genes correlated with CO_2 concentrations but not N_2O concentrations (Figure 5). The lack of association with N_2O is unsurprising since the denitrifier community composition included the suite of genes involved in the reduction of NO_3^- to N_2, with N_2O as an intermediate product that could be consumed before detection via gas chromatography. The association between denitrification and CO_2 production is likely the result of heterotrophic denitrification, where organic matter is oxidized to CO_2 with NO_3^- as an electron acceptor (Dlamini et al. 2020). Heterotrophic denitrification is typically a facultative process, found in organisms with the ability to respire aerobically when O_2 is available, and also use NO_3^- to respire anaerobically when O_2 availability decreases (Tiedje et al. 1989). A denitrification community-level response to soil hydrologic history and experimental drying/wetting has also

been observed in a previous incubation experiment (Peralta et al. 2013). The lack of differences in denitrification functional gene composition across histories and treatments observed here may be explained by the diversity of denitrifiers and their O_2 response phenotypes, and the variability of O_2 concentrations in soil microenvironments (Rohe et al. 2021; Wallenstein et al. 2006; Ji et al. 2015).

Methanogenesis

Our results showed a strong influence of hydrologic history on methanogen functional gene composition (Figure 5, Appendix S1: Table S7), which supports the classical view of methanogenesis as a specialized and strictly anaerobic metabolism, maintained in the historically wet (i.e., low O_2) field conditions (Lyu et al. 2018). The structure-function analysis (based on DBPLSR) provides another line of evidence that hydrologic history influenced CH_4 production, where methanogen functional gene composition explained a greater proportion of variance in CH_4 production at the start of the experiment than at the end of the experiment (Appendix S1: Table S11). Despite the lack of treatment effects on methanogen functional gene composition, CH_4 fluxes did respond to hydrologic treatments, indicating changes in methanogen activity were used to respond to the short-term hydrologic press disturbance.

Mismatch between microbial community composition and greenhouse gas function

The DNA-based functional gene composition explained more variance in GHG fluxes measured at the beginning than at the end of the experiment. Hydrologic history influenced wetland soil microbial community composition more than contemporary treatments. The decrease in the strength of structure-function associations from the beginning to the end of the

645 experiment could be due to the DNA-based molecular measurement providing insight into
646 historical and integrated environmental conditions, rather than contemporary changes to redox
647 conditions. For example, DNA from dormant and dead cells contributes to DNA-based
648 community composition, and these relic signatures are more indicative of past than present
649 conditions (Lennon et al. 2018). Changes to functional gene composition over the eight-week
650 experiment may have been obscured by the stable pool of dormant and relic DNA, thereby
651 weakening structure-function relationships, as observed here for CH_4 ~ methanogenesis, CO_2 ~
652 central carbohydrate metabolism, and CO_2 ~ CcO (Appendix S1: Table S11).
653 Another explanation for the decreased structure-function associations could be the
654 differences in temporal resolution between DNA-based molecular methods and *in situ* GHG
655 measurements. Differential gene expression can substantially alter CH_4 yields (Shi et al. 2014).
656 Protein expression and activity may be altered in response to O_2 concentrations (e.g., Lynch and
657 Lin 1996, reviewed in Saleh-Lakha et al. 2005). These changes to gene expression and protein
658 activity could alter GHG production rapidly, while changes to DNA abundance could alter GHG
659 production over multiple microbial generations. Mesocosm microbial communities in the present
660 study likely responded to experimental treatments (hydrology and plant presence or absence) by
661 altering gene expression and protein activity. Changes to functional gene abundance were likely
662 difficult to detect after eight weeks using DNA-based methods, hence the weakening of
663 structure-function relationships in CH_4 and CO_2 production at the end of the experiment.
664
665 *Limitations*
666 While this study provides valuable insights into the interplay between hydrology, plant
667 presence, and microbial communities, several limitations should be considered when interpreting

the results. First, the mesocosm setup, while necessary for experimental treatments, differs from wetland conditions. The experiment was conducted in a covered hoop house that prevented natural precipitation and altered light availability. Soil sampling may have altered soil structure, and mesocosms were disconnected from groundwater and deeper soil layers that may contribute to GHG emissions (Ball 2013; Sadat-Noori et al. 2016; Nikolenko et al. 2019). These factors could cause microbial responses to similar disturbances to differ in the field.

Finally, this study manipulated soils from a single restored coastal plain wetland. There are important differences between this restored wetland and remnant wetlands that restrict the generalization of results. The top 30 cm of soil were homogenized by decades of tillage (Hopfensperger et al. 2014). This likely reduced soil carbon storage, and 12 years post-restoration (at time of sampling), soil carbon storage likely lagged behind comparable remnant wetlands (Moreno-Mateos et al. 2012). Similarly, nitrogen storage and plant community structure in restored wetlands often recover but plateau below pre-degradation levels, representing an alternative stable state (Moreno-Mateos et al. 2012). Therefore, responses to hydrologic manipulation and loss of vegetation observed in the present study may vary from remnant wetland responses to similar disturbances. Increased restoration area (≥ 100 ha) and hydrologic connectivity are known to increase wetland restoration success (Moreno-Mateos et al. 2012). Both these features are present at the TOWeR site in the present study, and GHG flux responses to mesocosm hydrologic manipulation further underscore the importance of hydrology in wetland GHG function.

Conclusions

The long-term hydrologic history of a wetland shapes the resident microbial community, fostering a high degree of resistance to short-term hydrologic disturbances and loss of vegetation. While microbial community composition remained largely stable, we observed shifts in microbial function in response to short-term hydrologic manipulations. Dry treatment favored CO_2 production, and wet treatment favored CH_4 emissions. Our findings highlight the need to incorporate historical hydrologic conditions into models predicting wetland greenhouse gas emissions. Further research focusing on the interplay of soil history, short-term soil redox shifts, and plant-microbe interactions will be crucial for developing effective wetland management and climate change mitigation strategies.

Acknowledgments

We thank J. LeCrone, L. Armstrong, M. Stillwagon, G. Gunderson, C. Eakins, J. Basco, and C. Bledsoe for field and laboratory assistance. We thank J. Gill and the ECU grounds crew for their efforts in maintaining the grounds surrounding the shade house. We also thank M. Muscarella for contributions to microbiome analyses and anonymous reviewers for feedback on earlier versions of this manuscript. This work was supported by the National Science Foundation (Graduate Research Fellowship Program [GRFP] grant to R.B.B. and grant DEB #1845845 and CNH2 #2009185 to A.L.P.). This material is based upon work supported by the National Science Foundation under grant no. DGE-2125684. Any opinions, findings, and conclusions or recommendations expressed in this material are those of the author(s) and do not necessarily reflect the views of the National Science Foundation. The metagenomes were produced by the DOE JGI under the Community Science Program (CSP) (JGI CSP grant 503952). The work

conducted by the DOE JGI, a DOE Office of Science User Facility, is supported under contract DE-AC02-05CH11231.

Conflict of Interest Statement

The authors report no conflicts of interest.

References

Albuquerque, Luciana, Luís França, Fred A. Rainey, Peter Schumann, M. Fernanda Nobre, and Milton S. da Costa. 2011. "Gaiella Occulta Gen. Nov., Sp. Nov., a Novel Representative of a Deep Branching Phylogenetic Lineage within the Class Actinobacteria and Proposal of Gaiellaceae Fam. Nov. and Gaiellales Ord. Nov." *Systematic and Applied Microbiology* 34 (8): 595–99. https://doi.org/10.1016/j.syapm.2011.07.001.

Apprill, Amy, Sean Mcnally, Rachel Parsons, and Laura Weber. 2015. "Minor Revision to V4 Region SSU rRNA 806R Gene Primer Greatly Increases Detection of SAR11 Bacterioplankton." *Aquatic Microbial Ecology* 75 (2): 129–37. https://doi.org/10.3354/ame01753.

Apurv, Tushar, and Ximing Cai. 2021. "Regional Drought Risk in the Contiguous United States." *Geophysical Research Letters* 48 (5): e2020GL092200. https://doi.org/10.1029/2020GL092200.

Ardón, Marcelo, Jennifer L. Morse, Benjamin P. Colman, and Emily S. Bernhardt. 2013. "Drought-Induced Saltwater Incursion Leads to Increased Wetland Nitrogen Export." *Global Change Biology* 19 (10): 2976–85. https://doi.org/10.1111/gcb.12287.

Ardón, Marcelo, Jennifer L. Morse, Martin W. Doyle, and Emily S. Bernhardt. 2010. "The Water Quality Consequences of Restoring Wetland Hydrology to a Large Agricultural Watershed in the Southeastern Coastal Plain." *Ecosystems* 13 (7): 1060–78. https://doi.org/10.1007/s10021-010-9374-x.

Ball, B. C. 2013. "Soil Structure and Greenhouse Gas Emissions: A Synthesis of 20 Years of Experimentation." *European Journal of Soil Science* 64 (3): 357–73. https://doi.org/10.1111/ejss.12013.

Barron, E.S.G. 1939. "Cellular Oxidation Systems." *Physiological Reviews* 19: 184–239.

Bartoń, Kamil. 2025. *MuMIn: Multi-Model Inference*. V. 1.48.11. Released April 1. https://cran.r-project.org/web/packages/MuMIn/index.html.

Bates, D, M Machler, B Bolker, and S Walker. 2015. "Fitting Linear Mixed-Effects Models Using Lme4." *Journal of Statistical Software* 67 (1): 1–48. https://doi.org/10.18637/jss.v067.i01.

Blanca, María J., Rafael Alarcón, Jaume Arnau, Roser Bono, and Rebecca Bendayan. 2017. "Non-Normal Data: Is ANOVA Still a Valid Option?" *Psicothema* 29 (4): 552–57. https://doi.org/10.7334/psicothema2016.383.

Boj, Eva, Adria Caballe, Pedro Delicado, and Josep Fortiana. 2024. *Dbstats: Distance-Based Statistics Version 2.0.2 from CRAN*. Released. https://CRAN.R-project.org/package=dbstats.

Bridgham, Scott D., Hinsby Cadillo-Quiroz, Jason K. Keller, and Qianlai Zhuang. 2013. "Methane Emissions from Wetlands: Biogeochemical, Microbial, and Modeling Perspectives from Local to Global Scales." *Global Change Biology* 19 (5): 1325–46. https://doi.org/10.1111/gcb.12131.

Burgin, Amy J, Wendy H Yang, Stephen K Hamilton, and Whendee L Silver. 2011. "Beyond Carbon and Nitrogen: How the Microbial Energy Economy Couples Elemental Cycles in Diverse Ecosystems." *Frontiers in Ecology and the Environment* 9 (1): 44–52. https://doi.org/10.1890/090227.

Cadier, Charles, Elisa Bayraktarov, Renee Piccolo, and Maria Fernanda Adame. 2020. "Indicators of Coastal Wetlands Restoration Success: A Systematic Review." *Frontiers in Marine Science* 7 (December). https://doi.org/10.3389/fmars.2020.600220.

Caporaso, J Gregory, Christian L Lauber, William a Walters, et al. 2012. "Ultra-High-Throughput Microbial Community Analysis on the Illumina HiSeq and MiSeq Platforms." *The ISME Journal* 6 (8): 1621–24. https://doi.org/10.1038/ismej.2012.8.

Carmichael, M. J., E. S. Bernhardt, S. L. Bräuer, and W. K. Smith. 2014. "The Role of Vegetation in Methane Flux to the Atmosphere: Should Vegetation Be Included as a Distinct Category in the Global Methane Budget?" *Biogeochemistry* 119 (1–3): 1–24. https://doi.org/10.1007/s10533-014-9974-1.

Chanton, Jeffrey P. 2005. "The Effect of Gas Transport on the Isotope Signature of Methane in Wetlands." *Organic Geochemistry* 36 (5): 753–68. https://doi.org/10.1016/j.orggeochem.2004.10.007.

Chen, I-Min A., Victor M. Markowitz, Ken Chu, et al. 2017. "IMG/M: Integrated Genome and Metagenome Comparative Data Analysis System." *Nucleic Acids Research* 45 (D1): D507–16. https://doi.org/10.1093/nar/gkw929.

Christiansen, Jesper Riis, David Levy-Booth, Cindy E. Prescott, and Sue J. Grayston. 2016. "Microbial and Environmental Controls of Methane Fluxes Along a Soil Moisture Gradient in a Pacific Coastal Temperate Rainforest." *Ecosystems* 19 (7): 1255–70. https://doi.org/10.1007/s10021-016-0003-1.

Conrad, Ralf. 2009. "The Global Methane Cycle: Recent Advances in Understanding the Microbial Processes Involved." *Environmental Microbiology Reports* 1 (5): 285–92. https://doi.org/10.1111/j.1758-2229.2009.00038.x.

Dlamini, J. C., D. Chadwick, J. M. B. Hawkins, et al. 2020. "Evaluating the Potential of Different Carbon Sources to Promote Denitrification." *The Journal of Agricultural Science* 158 (3): 194–205. https://doi.org/10.1017/S0021859620000520.

Easterling, D. R., J. R. Arnold, T. Knutson, et al. 2017. "Precipitation Change in the United States." Vol. 1. https://doi.org/10.7930/J0H993CC.

Esposti, Mauro Degli. 2020. "On the Evolution of Cytochrome Oxidases Consuming Oxygen." *Biochimica et Biophysica Acta (BBA) - Bioenergetics* 1861 (12): 148304. https://doi.org/10.1016/j.bbabio.2020.148304.

Fairbairn, Linden, Fereidoun Rezanezhad, Mehdi Gharasoo, et al. 2023. "Relationship between Soil CO2 Fluxes and Soil Moisture: Anaerobic Sources Explain Fluxes at High Water Content." *Geoderma* 434 (June): 116493. https://doi.org/10.1016/j.geoderma.2023.116493.

Ferry, James G. 2011. "Fundamentals of Methanogenic Pathways That Are Key to the Biomethanation of Complex Biomass." *Current Opinion in Biotechnology*, Energy biotechnology – Environmental biotechnology, vol. 22 (3): 351–57. https://doi.org/10.1016/j.copbio.2011.04.011.

Finlay, Colin G., and Ariane L. Peralta. 2025. "Hydrologic History and Flooding Pulses Control Iron and Sulfur Metabolic Composition with Variable Associations to Greenhouse Gas Production in a Coastal Wetland Mesocosm Experiment." Preprint, bioRxiv, March 5. https://doi.org/10.1101/2025.03.03.641170.

Fluet-Chouinard, Etienne, Benjamin D. Stocker, Zhen Zhang, et al. 2023. "Extensive Global Wetland Loss over the Past Three Centuries." *Nature* 614 (7947): 7947. https://doi.org/10.1038/s41586-022-05572-6.

Freddi, Luca, Jorge A. de la Garza-García, Sascha Al Dahouk, Alessandra Occhialini, and Stephan Köhler. 2023. "Brucella Spp. Are Facultative Anaerobic Bacteria under Denitrifying Conditions." *Microbiology Spectrum* 11 (6): e02767-23. https://doi.org/10.1128/spectrum.02767-23.

Fukami, Tadashi, Ian A. Dickie, J. Paula Wilkie, et al. 2010. "Assembly History Dictates Ecosystem Functioning: Evidence from Wood Decomposer Communities." *Ecology Letters* 13 (6): 675–84. https://doi.org/10.1111/j.1461-0248.2010.01465.x.

Fuss, Roland, and Roman Hueppi. 2024. *Gasfluxes: Greenhouse Gas Flux Calculation from Chamber Measurements*. V. 0.6-2. Released January 8. https://cran.r-project.org/web/packages/gasfluxes/index.html.

Glassman, Sydney I., and Jennifer B. H. Martiny. 2018. "Broadscale Ecological Patterns Are Robust to Use of Exact Sequence Variants versus Operational Taxonomic Units." *mSphere* 3 (4): e00148-18. https://doi.org/10.1128/mSphere.00148-18.

Gorsky, A. L., G. A. Racanelli, A. C. Belvin, and R. M. Chambers. 2019. "Greenhouse Gas Flux from Stormwater Ponds in Southeastern Virginia (USA)." *Anthropocene* 28. https://doi.org/10.1016/j.ancene.2019.100218.

Griffith, Jerry A., Stephen V. Stehman, and Thomas R. Loveland. 2003. "Landscape Trends in Mid-Atlantic and Southeastern United States Ecoregions." *Environmental Management* 32 (5): 572–88. https://doi.org/10.1007/s00267-003-0078-2.

Griffiths, B. S., P. D. Hallett, H. L. Kuan, A. S. Gregory, C. W. Watts, and A. P. Whitmore. 2008. "Functional Resilience of Soil Microbial Communities Depends on Both Soil Structure and Microbial Community Composition." *Biology and Fertility of Soils* 44 (5): 745–54. https://doi.org/10.1007/s00374-007-0257-z.

Griffiths, Bryan S., and Laurent Philippot. 2013. "Insights into the Resistance and Resilience of the Soil Microbial Community." *FEMS Microbiology Reviews* 37 (2): 112–29. https://doi.org/10.1111/j.1574-6976.2012.00343.x.

Havlicek, Larry L., and Nancy L. Peterson. 1974. "Robustness of the T Test: A Guide for Researchers on Effect of Violations of Assumptions." *Psychological Reports* 34 (3_suppl): 1095–114. https://doi.org/10.2466/pr0.1974.34.3c.1095.

Hernández, Marcela, Ralf Conrad, Melanie Klose, Ke Ma, and Yahai Lu. 2017. "Structure and Function of Methanogenic Microbial Communities in Soils from Flooded Rice and Upland Soybean Fields from Sanjiang Plain, NE China." *Soil Biology and Biochemistry* 105 (February): 81–91. https://doi.org/10.1016/j.soilbio.2016.11.010.

Hoffmann, Mathias, Natalia Pehle, Vytas Huth, Nicole Jurisch, Michael Sommer, and Jürgen Augustin. 2018. "A Simple Method to Assess the Impact of Sealing, Headspace Mixing and Pressure Vent on Airtightness of Manually Closed Chambers." *Journal of Plant Nutrition and Soil Science* 181 (1): 36–40. https://doi.org/10.1002/jpln.201600299.

Hopfensperger, Kristine N., Amy J. Burgin, Valerie A. Schoepfer, and Ashley M. Helton. 2014. "Impacts of Saltwater Incursion on Plant Communities, Anaerobic Microbial Metabolism, and Resulting Relationships in a Restored Freshwater Wetland." *Ecosystems* 17 (5): 792–807. https://doi.org/10.1007/s10021-014-9760-x.

Hu, Qiwu, Jiayan Cai, Bo Yao, Qin Wu, Yeqiao Wang, and Xingliang Xu. 2015. "Plant-Mediated Methane and Nitrous Oxide Fluxes from a Carex Meadow in Poyang Lake during Drawdown Periods." *Plant and Soil*, ahead of print. https://doi.org/10.1007/s11104-015-2733-9.

Huntemann, Marcel, Natalia N. Ivanova, Konstantinos Mavromatis, et al. 2016. "The Standard Operating Procedure of the DOE-JGI Metagenome Annotation Pipeline (MAP v.4)." *Standards in Genomic Sciences* 11 (1): 17. https://doi.org/10.1186/s40793-016-0138-x.

Hurvich, C, and C Tsai. 1993. "A CORRECTED AKAIKE INFORMATIONON CRITERION FOR VECTOR AUTOREGRESSIVE MODEL SELECTION." *Journal of Time Series Analysis* 14 (3): 271–79.

IPCC. 2023. *Climate Change 2023: Synthesis Report. Contribution of Working Groups I, II and III to the Sixth Assessment Report of the Intergovernmental Panel on Climate Change*. IPCC. https://dx.doi.org/10.59327/IPCC/AR6-9789291691647.

Jabłońska, Jagoda, and Dan S. Tawfik. 2019. "The Number and Type of Oxygen-Utilizing Enzymes Indicates Aerobic vs. Anaerobic Phenotype." *Free Radical Biology and Medicine*, Early Life on Earth and Oxidative Stress, vol. 140 (August): 84–92. https://doi.org/10.1016/j.freeradbiomed.2019.03.031.

Jenkinson, B. J., and D. P. Franzmeier. 2006. "Development and Evaluation of Iron-Coated Tubes That Indicate Reduction in Soils." *Soil Science Society of America Journal* 70 (1): 183–91. https://doi.org/10.2136/sssaj2004.0323.

Ji, Bin, Kai Yang, Lei Zhu, et al. 2015. "Aerobic Denitrification: A Review of Important Advances of the Last 30 Years." *Biotechnology and Bioprocess Engineering* 20 (4): 643–51. https://doi.org/10.1007/s12257-015-0009-0.

Johnston, Eric R., Janet K. Hatt, Zhili He, et al. 2019. "Responses of Tundra Soil Microbial Communities to Half a Decade of Experimental Warming at Two Critical Depths." *Proceedings of the National Academy of Sciences* 116 (30): 15096–105. https://doi.org/10.1073/pnas.1901307116.

Kim, Seon Young, Seung Hoon Lee, Chris Freeman, Nathalie Fenner, and Hojeong Kang. 2008. "Comparative Analysis of Soil Microbial Communities and Their Responses to the Short-Term Drought in Bog, Fen, and Riparian Wetlands." *Soil Biology and Biochemistry* 40 (11): 2874–80. https://doi.org/10.1016/j.soilbio.2008.08.004.

Kimball, Spencer, Peter Mattis, Michael Natterer, and Jehan. 2014. *GIMP*. V. v2.8.14. Released. https://www.gimp.org/.

Kingsford, Richard T., Alberto Basset, and Leland Jackson. 2016. "Wetlands: Conservation's Poor Cousins." *Aquatic Conservation: Marine and Freshwater Ecosystems* 26 (5): 892–916. https://doi.org/10.1002/aqc.2709.

König, Sara, Anja Worrich, Thomas Banitz, et al. 2018. "Functional Resistance to Recurrent Spatially Heterogeneous Disturbances Is Facilitated by Increased Activity of Surviving Bacteria in a Virtual Ecosystem." *Frontiers in Microbiology* 9 (April). https://doi.org/10.3389/fmicb.2018.00734.

Kozich, James J., Sarah L. Westcott, Nielson T. Baxter, Sarah K. Highlander, and Patrick D. Schloss. 2013. "Development of a Dual-Index Sequencing Strategy and Curation Pipeline for Analyzing Amplicon Sequence Data on the Miseq Illumina Sequencing Platform." *Applied and Environmental Microbiology* 79 (17): 5112–20. https://doi.org/10.1128/AEM.01043-13.

Kuzyakov, Yakov. 2010. "Soil Biology & Biochemistry Priming Effects : Interactions between Living and Dead Organic Matter." *Soil Biology and Biochemistry* 42 (9): 1363–71. https://doi.org/10.1016/j.soilbio.2010.04.003.

Lee, Hyosun, Dong-Uk Kim, Suyeon Lee, et al. 2017. "Reyranella Terrae Sp. Nov., Isolated from an Agricultural Soil, and Emended Description of the Genus Reyranella."

International Journal of Systematic and Evolutionary Microbiology 67 (6): 2031–35. https://doi.org/10.1099/ijsem.0.001913.

Lennon, J. T., S. D. W. Frost, N. K. Nguyen, A. L. Peralta, A. R. Place, and K. K. Treseder. 2023. "Microbiology and Climate Change: A Transdisciplinary Imperative." *mBio* 14 (1): e03335-22. https://doi.org/10.1128/mbio.03335-22.

Lennon, J. T., M. E. Muscarella, S. A. Placella, and B. K. Lehmkuhl. 2018. "How, When, and Where Relic DNA Affects Microbial Diversity." *mBio* 9 (3): 10.1128/mbio.00637-18. https://doi.org/10.1128/mbio.00637-18.

Liu, Yu-Rong, Manuel Delgado-Baquerizo, Ziming Yang, Jiao Feng, Jun Zhu, and Qiaoyun Huang. 2020. "Microbial Taxonomic and Functional Attributes Consistently Predict Soil CO2 Emissions across Contrasting Croplands." *Science of The Total Environment* 702 (February): 134885. https://doi.org/10.1016/j.scitotenv.2019.134885.

Luan, Junwei, and Jianghua Wu. 2014. "Gross Photosynthesis Explains the 'artificial Bias' of Methane Fluxes by Static Chamber (Opaque versus Transparent) at the Hummocks in a Boreal Peatland." *Environmental Research Letters* 9 (10). https://doi.org/10.1088/1748-9326/9/10/105005.

Lynch, A S, and E C Lin. 1996. "Transcriptional Control Mediated by the ArcA Two-Component Response Regulator Protein of Escherichia Coli: Characterization of DNA Binding at Target Promoters." *Journal of Bacteriology* 178 (21): 6238–49. https://doi.org/10.1128/jb.178.21.6238-6249.1996.

Lyu, Zhe, Nana Shao, Taiwo Akinyemi, and William B. Whitman. 2018. "Methanogenesis." *Current Biology* 28 (13): R727–32. https://doi.org/10.1016/j.cub.2018.05.021.

Maietta, Christine E., Kelly L. Hondula, C. Nathan Jones, and Margaret A. Palmer. 2020. "Hydrological Conditions Influence Soil and Methane-Cycling Microbial Populations in Seasonally Saturated Wetlands." *Frontiers in Environmental Science* 8 (November). https://doi.org/10.3389/fenvs.2020.593942.

Markowitz, Victor M., I-Min A. Chen, Ken Chu, et al. 2014. "IMG/M 4 Version of the Integrated Metagenome Comparative Analysis System." *Nucleic Acids Research* 42 (D1): D568–73. https://doi.org/10.1093/nar/gkt919.

Marschner, Petra. 2021. "Processes in Submerged Soils – Linking Redox Potential, Soil Organic Matter Turnover and Plants to Nutrient Cycling." *Plant and Soil* 464 (1): 1–12. https://doi.org/10.1007/s11104-021-05040-6.

Martínez-Espinosa, Columba, Sabine Sauvage, Ahmad Al Bitar, Pamela A. Green, Charles J. Vörösmarty, and José Miguel Sánchez-Pérez. 2021. "Denitrification in Wetlands: A Review towards a Quantification at Global Scale." *Science of The Total Environment* 754 (February): 142398. https://doi.org/10.1016/j.scitotenv.2020.142398.

McDonald, I R, and J C Murrell. 1997. "The Methanol Dehydrogenase Structural Gene mxaF and Its Use as a Functional Gene Probe for Methanotrophs and Methylotrophs." *FEMS Microbiology Letters* 156 (8): 205–10.

Mcleod, Elizabeth, Gail L Chmura, Steven Bouillon, et al. 2011. "A Blueprint for Blue Carbon: Toward an Improved Understanding of the Role of Vegetated Coastal Habitats in Sequestering CO2." *Frontiers in Ecology and the Environment* 9 (10): 552–60. https://doi.org/10.1890/110004.

Mehlich, A. 1984. "Mehlich 3 Soil Test Extractant: A Modification of Mehlich 2 Extractant." *Communications in Soil Science and Plant Analysis* 15 (12): 1409–16. https://doi.org/10.1080/00103628409367568.

Mitsch, William J., Blanca Bernal, and Maria E. Hernandez. 2015. "Ecosystem Services of Wetlands." *International Journal of Biodiversity Science, Ecosystem Services & Management* 11 (1): 1–4. https://doi.org/10.1080/21513732.2015.1006250.

Mitsch, William J., Blanca Bernal, Amanda M. Nahlik, et al. 2013. "Wetlands, Carbon, and Climate Change." *Landscape Ecology* 28 (4): 583–97. https://doi.org/10.1007/s10980-012-9758-8.

Mitsch, William J., and James G. Gosslink. 2007. *Wetlands*. 4th ed. John Wiley & Sons.

Moreno-Mateos, David, Mary E. Power, Francisco A. Comín, and Roxana Yockteng. 2012. "Structural and Functional Loss in Restored Wetland Ecosystems." *PLOS Biology* 10 (1): e1001247. https://doi.org/10.1371/journal.pbio.1001247.

Morse, Jennifer L., Marcelo Ardón, and Emily S. Bernhardt. 2012. "Greenhouse Gas Fluxes in Southeastern U.S. Coastal Plain Wetlands under Contrasting Land Uses." *Ecological Applications* 22 (1): 264–80. https://doi.org/10.1890/11-0527.1.

Mylavarapu, Rao, Tom Obreza, Kelly Morgan, George Hochmuth, Vimala Nair, and Alan Wright. 2014. "Extraction of Soil Nutrients Using Mehlich-3 Reagent for Acid-Mineral Soils of Florida." *University of Florida. Institute of Food and Agricultural Science*, no. SL407: 1–7.

Nijs, Evy A. de, Lettice C. Hicks, Ainara Leizeaga, Albert Tietema, and Johannes Rousk. 2019. "Soil Microbial Moisture Dependences and Responses to Drying–Rewetting: The Legacy of 18 Years Drought." *Global Change Biology* 25 (3): 1005–15. https://doi.org/10.1111/gcb.14508.

Nikolenko, Olha, Philippe Orban, Anna Jurado, et al. 2019. "Dynamics of Greenhouse Gases in Groundwater: Hydrogeological and Hydrogeochemical Controls." *Applied Geochemistry* 105 (June): 31–44. https://doi.org/10.1016/j.apgeochem.2019.04.009.

Northfield, Tobin D., Gretchen B. Snyder, Anthony R. Ives, and William E. Snyder. 2010. "Niche Saturation Reveals Resource Partitioning among Consumers." *Ecology Letters* 13 (3): 338–48. https://doi.org/10.1111/j.1461-0248.2009.01428.x.

Oksanen, Jari. 2015. *Vegan : Ecological Diversity*. 1 (2): 1–12. https://doi.org/10.1029/2006JF000545.

Parada, Alma E., David M. Needham, and Jed A. Fuhrman. 2016. "Every Base Matters: Assessing Small Subunit rRNA Primers for Marine Microbiomes with Mock Communities, Time Series and Global Field Samples." *Environmental Microbiology* 18 (5): 1403–14. https://doi.org/10.1111/1462-2920.13023.

Patel, Kajal, Meenakshi Chaurasia, InduTripathi, and Shilpi Nagar. 2021. "Wetland Conservation and Restoration." In *Wetlands Conservation*. John Wiley & Sons, Ltd. https://doi.org/10.1002/9781119692621.ch13.

Peralta, Ariane L., Regina B. Bledsoe, Mario E. Muscarella, et al. 2020. "Metagenomes from Experimental Hydrologic Manipulation of Restored Coastal Plain Wetland Soils (Tyrell County, North Carolina)." *Microbiology Resource Announcements* 9 (41). https://doi.org/10.1128/MRA.00882-20.

Peralta, Ariane L., Sarah Ludmer, and Angela D. Kent. 2013. "Hydrologic History Influences Microbial Community Composition and Nitrogen Cycling under Experimental Drying/Wetting Treatments." *Soil Biology and Biochemistry* 66 (November): 29–37. https://doi.org/10.1016/j.soilbio.2013.06.019.

Peralta, Ariane L, Sarah Ludmer, Jeffrey W Matthews, and Angela D Kent. 2014. "Bacterial Community Response to Changes in Soil Redox Potential along a Moisture Gradient in

Restored Wetlands." *Ecological Engineering* 73: 246–53. https://doi.org/10.1016/j.ecoleng.2014.09.047.

Peralta, Ariane L, Diana Stuart, Angela D Kent, and Jay T Lennon. 2014. "A Social–Ecological Framework for 'Micromanaging' Microbial Services." *Frontiers in Ecology and the Environment* 12 (9): 524–31. https://doi.org/10.1890/130308.

Philippot, Laurent, Bryan S. Griffiths, and Silke Langenheder. 2021. "Microbial Community Resilience across Ecosystems and Multiple Disturbances." *Microbiology and Molecular Biology Reviews* 85 (2): 10.1128/mmbr.00026-20. https://doi.org/10.1128/mmbr.00026-20.

Philippot, Laurent, Jos M. Raaijmakers, Philippe Lemanceau, and Wim H. Van Der Putten. 2013. "Going Back to the Roots: The Microbial Ecology of the Rhizosphere." *Nature Reviews Microbiology* 11 (11): 789–99. https://doi.org/10.1038/nrmicro3109.

Pimm, Stuart L. 1984. "The Complexity and Stability of Ecosystems." *Nature* 307 (5949): 321–26. https://doi.org/10.1038/307321a0.

Potapov, Peter, Matthew C. Hansen, Amy Pickens, et al. 2022. "The Global 2000-2020 Land Cover and Land Use Change Dataset Derived From the Landsat Archive: First Results." *Frontiers in Remote Sensing* 3 (April). https://doi.org/10.3389/frsen.2022.856903.

Quast, Christian, Elmar Pruesse, Pelin Yilmaz, et al. 2013. "The SILVA Ribosomal RNA Gene Database Project: Improved Data Processing and Web-Based Tools." *Nucleic Acids Research* 41 (D1): 590–96. https://doi.org/10.1093/nar/gks1219.

R Core Team. 2024. *R: A Language and Environment for Statistical Computing*. V. 4.4.2 (2024-10-31) -- "Pile of Leaves." R Foundation for Statistical Computing, released. https://www.R-project.org/.

Rabenhorst, Martin C. 2008. "Protocol for Using and Interpreting IRIS Tubes." *Soil Survey Horizons* 49 (3): 74–77.

Ran, Yiguo, Shengjun Wu, Kai Zhu, Wenjuan Li, Zhimei Liu, and Ping Huang. 2020. "Soil Types Differentiated Their Responses of Aggregate Stability to Hydrological Stresses at the Riparian Zones of the Three Gorges Reservoir." *Journal of Soils and Sediments* 20 (2): 951–62. https://doi.org/10.1007/s11368-019-02410-7.

Ricks, Kevin D., and Anthony C. Yannarell. 2023. "Soil Moisture Incidentally Selects for Microbes That Facilitate Locally Adaptive Plant Response." *Proceedings of the Royal Society B: Biological Sciences* 290 (2001): 20230469. https://doi.org/10.1098/rspb.2023.0469.

Roberts, David W. 2023. *Labdsv: Ordination and Multivariate Analysis for Ecology*. V. 2.1-0. Released April 10. https://cran.r-project.org/web/packages/labdsv/index.html.

Rognes, Torbjørn, Tomáš Flouri, Ben Nichols, Christopher Quince, and Frédéric Mahé. 2016. "VSEARCH: A Versatile Open Source Tool for Metagenomics." *PeerJ* 4: e2584. https://doi.org/10.7717/peerj.2584.

Rohe, Lena, Bernd Apelt, Hans-Jörg Vogel, Reinhard Well, Gi-Mick Wu, and Steffen Schlüter. 2021. "Denitrification in Soil as a Function of Oxygen Availability at the Microscale." *Biogeosciences* 18 (3): 1185–201. https://doi.org/10.5194/bg-18-1185-2021.

Sadat-Noori, Mahmood, Damien T. Maher, and Isaac R. Santos. 2016. "Groundwater Discharge as a Source of Dissolved Carbon and Greenhouse Gases in a Subtropical Estuary." *Estuaries and Coasts* 39 (3): 639–56. https://doi.org/10.1007/s12237-015-0042-4.

Saleh-Lakha, Saleema, Michelle Miller, Rachel G. Campbell, et al. 2005. "Microbial Gene Expression in Soil: Methods, Applications and Challenges." *Journal of Microbiological Methods* 63 (1): 1–19. https://doi.org/10.1016/j.mimet.2005.03.007.

Schielzeth, Holger, Niels J. Dingemanse, Shinichi Nakagawa, et al. 2020. "Robustness of Linear Mixed-Effects Models to Violations of Distributional Assumptions." *Methods in Ecology and Evolution* 11 (9): 1141–52. https://doi.org/10.1111/2041-210X.13434.

Schloss, Patrick D. 2021. "Amplicon Sequence Variants Artificially Split Bacterial Genomes into Separate Clusters." *mSphere* 6 (4): e00191-21. https://doi.org/10.1128/mSphere.00191-21.

Schloss, Patrick D., Sarah L. Westcott, Thomas Ryabin, et al. 2009. "Introducing Mothur: Open-Source, Platform-Independent, Community-Supported Software for Describing and Comparing Microbial Communities." *Applied and Environmental Microbiology* 75 (23): 7537–41. https://doi.org/10.1128/AEM.01541-09.

Schneider, Caroline A, Wayne S Rasband, and Kevin W Eliceiri. 2012. "NIH Image to ImageJ: 25 Years of Image Analysis." *Nature Methods* 9 (7): 671–75. https://doi.org/10.1038/nmeth.2089.

Schneider, Grant, Eric Chicken, and Rachel Becvarik. 2023. *NSM3: Functions and Datasets to Accompany Hollander, Wolfe, and Chicken - Nonparametric Statistical Methods, Third Edition*. V. 1.18. Released September 4. https://cran.r-project.org/web/packages/NSM3/index.html.

Seto, Mayumi, Risa Sasaki, Hideshi Ooka, and Ryuhei Nakamura. 2025. "Thermodynamics Underpinning the Microbial Community-Level Nitrogen Energy Metabolism." *Environmental Microbiology* 27 (2): e70055. https://doi.org/10.1111/1462-2920.70055.

Shade, Ashley, Hannes Peter, Steven D. Allison, et al. 2012. "Fundamentals of Microbial Community Resistance and Resilience." *Frontiers in Microbiology* 3 (December). https://doi.org/10.3389/fmicb.2012.00417.

Shi, Weibing, Christina D. Moon, Sinead C. Leahy, et al. 2014. "Methane Yield Phenotypes Linked to Differential Gene Expression in the Sheep Rumen Microbiome." *Genome Research* 24 (9): 1517–25. https://doi.org/10.1101/gr.168245.113.

Skeeter, Walker J., Jason C. Senkbeil, and David J. Keellings. 2019. "Spatial and Temporal Changes in the Frequency and Magnitude of Intense Precipitation Events in the Southeastern United States." *International Journal of Climatology* 39 (2): 768–82. https://doi.org/10.1002/joc.5841.

Spieles, Douglas J. 2022. "Wetland Construction, Restoration, and Integration: A Comparative Review." *Land* 11 (4): 554. https://doi.org/10.3390/land11040554.

Suhani, Ibha, Monika, Barkha Vaish, Pooja Singh, and Rajeev Pratap Singh. 2020. "Restoration, Construction, and Conservation of Degrading Wetlands: A Step Toward Sustainable Management Practices." In *Restoration of Wetland Ecosystem: A Trajectory Towards a Sustainable Environment*, edited by Atul Kumar Upadhyay, Ranjan Singh, and D. P. Singh. Springer. https://doi.org/10.1007/978-981-13-7665-8_1.

Sun, Haishu, Shengjun Xu, Shanghua Wu, et al. 2019. "Enhancement of Facultative Anaerobic Denitrifying Communities by Oxygen Release from Roots of the Macrophyte in Constructed Wetlands." *Journal of Environmental Management* 246 (September): 157–63. https://doi.org/10.1016/j.jenvman.2019.05.136.

Sundberg, Carina, Jenny S. Jenny, Karin Tonderski, and Per Eric Lindgren. 2007. "Overland Flow Systems for Treatment of Landfill Leachates-Potential Nitrification and Structure of

the Ammonia-Oxidising Bacterial Community during a Growing Season." *Soil Biology and Biochemistry* 39 (1): 127–38. https://doi.org/10.1016/j.soilbio.2006.06.016.

Terando, Adam J., Jennifer Costanza, Curtis Belyea, Robert R. Dunn, Alexa McKerrow, and Jaime A. Collazo. 2014. "The Southern Megalopolis: Using the Past to Predict the Future of Urban Sprawl in the Southeast U.S." *PLOS ONE* 9 (7): e102261. https://doi.org/10.1371/journal.pone.0102261.

Tiedje, J. M., A. J. Sexstone, T. B. Parkin, and N. P. Revsbech. 1984. "Anaerobic Processes in Soil." *Plant and Soil* 76 (1): 197–212. https://doi.org/10.1007/BF02205580.

Tiedje, James M., Stephen Simkins, and Peter M. Groffman. 1989. "Perspectives on Measurement of Denitrification in the Field Including Recommended Protocols for Acetylene-Based Methods." *Plant and Soil* 115 (2): 261–84. https://doi.org/10.1007/BF02202594.

Treseder, Kathleen K., Teri C. Balser, Mark A. Bradford, et al. 2012. "Integrating Microbial Ecology into Ecosystem Models: Challenges and Priorities." *Biogeochemistry* 109 (1): 7–18. https://doi.org/10.1007/s10533-011-9636-5.

Truu, Marika, Jaanis Juhanson, and Jaak Truu. 2009. "Microbial Biomass, Activity and Community Composition in Constructed Wetlands." *Science of The Total Environment* 407 (13): 3958–71. https://doi.org/10.1016/j.scitotenv.2008.11.036.

Voorde, Tess F. J. van de, Wim H. van der Putten, and T. Martijn Bezemer. 2011. "Intra- and Interspecific Plant–Soil Interactions, Soil Legacies and Priority Effects during Old-Field Succession." *Journal of Ecology* 99 (4): 945–53. https://doi.org/10.1111/j.1365-2745.2011.01815.x.

Wallenstein, Matthew D., David D. Myrold, Mary Firestone, and Mary Voytek. 2006. "Environmental Controls on Denitrifying Communities and Denitrification Rates: Insights from Molecular Methods." *Ecological Applications* 16 (6): 2143–52. https://doi.org/10.1890/1051-0761(2006)016%255B2143:ECODCA%255D2.0.CO;2.

Walz, Dieter. 1979. "Thermodynamics of Oxidation-Reduction Reactions and Its Application to Bioenergetics." *Biochimica et Biophysica Acta (BBA) - Reviews on Bioenergetics* 505 (3): 279–353. https://doi.org/10.1016/0304-4173(79)90007-7.

Zedler, Joy B., and Suzanne Kercher. 2005. "WETLAND RESOURCES: Status, Trends, Ecosystem Services, and Restorability." *Annual Review of Environment and Resources* 30 (Volume 30, 2005): 39–74. https://doi.org/10.1146/annurev.energy.30.050504.144248.

Zhao, Zhun, Peng Shi, Lulu Bai, et al. 2024. "Vegetation Patterns Affect Soil Aggregate Loss during Water Erosion." *Land Degradation & Development* 35 (3): 936–48. https://doi.org/10.1002/ldr.4962.

1117 **Tables**

1118 **Table 1**. Soil chemical and physical properties measured after eight weeks of hydrologic

1119 manipulation.

Treatment	Dry		Interim		Wet	
Plant	No Plant	Plant	No Plant	Plant	No Plant	Plant
Moisture (%)	39 ± 0.31	14 ± 0.03	19 ± 0.16	13 ± 0.02	29 ± 0.23	62 ± 0.07
pH	5.31 ± 0.11	5.31 ± 0.09	5.4 ± 0.16	5.35 ± 0.1	5.55 ± 0.15	5.41 ± 0.17
NH_4^+ mg L^{-1}	0.39 ± 0.07	0.27 ± 0.04	0.26 ± 0.1	0.19 ± 0.02	0.77 ± 0.76	0.39 ± 0.42
NO_3^- mg L^{-1}	0.08 ± 0.07	MDL	0.25 ± 0.38	MDL	0.01 ± 0.0005	MDL
Total C (%)	4.63 ± 0.78	4.63 ± 0.81	4.48 ± 0.32	4.37 ± 0.52	4.91 ± 0.92	4.68 ± 0.74
Total N (%)	0.22 ± 0.03	0.22 ± 0.03	0.22 ± 0.01	0.21 ± 0.03	0.24 ± 0.04	0.23 ± 0.03
P ppm	21.00 ± 4.14	20.41 ± 4.4	23.58 ± 8.87	22.83 ± 8.37	23.16 ± 5.98	23 ± 5.79
K ppm	33.66 ± 5.97	30.25 ± 10.31	39.5 ± 11.44	26.75 ± 3.04	46.16 ± 16.02	34.25 ± 10.78
Mg ppm	77.58 ± 6.46	74.66 ± 11.43	86 ± 22.33	78.66 ± 16.47	89.25 ± 16.85	79.41 ± 18.8
S ppm	15.75 ± 1.94	15.33 ± 2.29	13.25 ± 1.25	12.16 ± 0.40	11.33 ± 1.21	11.5 ± 1.00
Fe ppm	252.66 ± 14.45	243.66 ± 17.06	275.33 ± 27.07	251.16 ± 37.6	306.83 ± 22.52	280.66 ± 40.71
Mn ppm	3.91 ± 1.15	3.41 ± 0.97	4.33 ± 1.16	4.58 ± 1.31	5.83 ± 1.32	5.58 ± 2.05
Humic matter (%)	2.35 ± 0.19	2.17 ± 0.14	2.04 ± 0.29	2.28 ± 0.22	1.98 ± 0.422	1.96 ± 0.43

1120 Notes: Average (mean ± standard deviation) by hydrologic treatment and plant status are

1121 reported to show differences among groups.

1122 Abbreviations: NH_4^+ = ammonium, NO_3^- = nitrate, MDL = below detection limit, C = carbon, N

1123 = nitrogen, P = phosphorus, K = potassium, Mg = magnesium, S = sulfur, Fe = iron, Mn =

1124 manganese, ppm = parts per million.

1125

1126

1127

Figures captions

Figure 1. Field site and mesocosm set-up. Wetland mesocosms sourced from the Timberlake Observatory for Wetland Restoration (image modified with permission from Ardón et al., 2013) (a). Aerial view of wetland mesocosm setup, where the left side of the box represents plant treatment, and the right side represents no plant treatment, separated by a stainless mesh divider ((b), top, photo credit: R. Bledsoe). Collars were installed for measuring greenhouse gas concentrations. Also shown is a 1-liter bottle attached to each side of the mesocosm used to maintain water levels. Example of a wet treatment mesocosm with indicator of reduction in soils (IRIS) tubes installed ((b), middle, photo credit: R. Bledsoe). Example of mesocosm with prepared for greenhouse gas sampling ((b), bottom, photo credit: R. Bledsoe). Abbreviations: PP = Palmetto Peartree Preserve, PA = preservation area, TR = Timberlake Observatory for Wetland Restoration.

Figure 2. Indicator of reduction in soils (IRIS) tubes mesocosm image (photo credit: R. Bledsoe) (a), IRIS tube example images (photo credit: R. Bledsoe) (b), and boxplots summarizing redox status at the beginning and end of the experiment (c). Percent paint removed from IRIS tubes at the start of the experiment (week 0) and the end of the experiment (week 8). Example IRIS tubes used for ImageJ analysis post-incubation (b) with plant icons crossed out represent IRIS tubes from mesocosms with plants removed, and plant icons represent IRIS tubes from mesocosms with plants present. Box plots summarize percent paint removed from IRIS tubes at start (week 0) and finish (week 8) of experimental incubation. Color represents hydrologic treatment: brown indicates dry, light blue indicates interim, and dark blue indicates wet. Individual samples are plotted as points and colored according to their hydrologic treatment. Point shape represents

hydrologic history (square = dry history, triangle = interim history, circle = wet history). Closed points represent mesocosms with plants, while open points represent mesocosms without plants. Boxplots summarize median, first and third quartiles, and two whiskers extending |≤| 1.5 * interquartile range.

Figure 3. Greenhouse gas fluxes in dry, interim, and wet hydrologic treatments. Fluxes are in milligrams of methane (CH_4) (a), carbon dioxide (CO_2) (b), and nitrous oxide (N_2O) (c) per square meter per hour (mg m^{-2} h^{-1}) and are compared for hydrologic treatments during the five time points. Individual samples are plotted as shapes and colored by hydrologic treatment (brown squares = dry, light blue triangles = interim, dark blue circles = wet). Point shape represents hydrologic history (square = dry history, triangle = interim history, circle = wet history). Closed points represent mesocosms with plants, while open points represent mesocosms without plants. Boxplots summarize the median, first and third quartiles, and two whiskers extending |≤| 1.5 * interquartile range. Asterisks represent significance levels of Dwass, Steel, Critchlow, and Fligner (SDCFlig) tests (****: $p \leq 0.0001$, ***: $p \leq 0.001$, **: $p \leq 0.01$, *: $p \leq 0.05$, no symbol: $p > 0.05$). An extreme outlier of 248 mg CH_4 m^{-2} h^{-1}, measured in a mesocosm from interim soil history and wet treatment with no plants on July 11th, was used in statistical calculations but not displayed in the plot to improve visualization of differences across treatments. Month names are abbreviated as follows: Jun = June, Jul = July, Aug = August.

Figure 4. Ordination based on a principal coordinates analysis (PCoA) depicting the composition of the bacterial and archaeal communities based on the 16S rRNA gene. Colors

1173 refer to hydrologic treatments: brown indicates dry, light blue indicates interim, and dark blue
1174 indicates wet. Shapes refer to the hydrologic history of the sample: a square indicates dry, a
1175 triangle indicates interim, and a circle indicates wet. Open shapes refer to samples from
1176 mesocosms without plants, while closed shapes refer to samples from mesocosms with plants.
1177 Labeled vectors represent relationships among soil physicochemical variables and the microbial
1178 community ordination, with $p \leq 0.05$, scaled by their correlation (using the *envfit* function).
1179 Abbreviations: CEC = cation exchange capacity, Fe = iron, S = sulfur, Cu = copper, Ca =
1180 calcium, Mn = manganese, Mg = magnesium, %C = percent carbon, %N = percent nitrogen.

1181

1182 **Figure 5.** Ordination based on a principal coordinates analysis (PCoA) depicting community
1183 composition of the functional gene modules. The PCoA ordination is based on the Bray-Curtis
1184 distance of relative abundance of functional genes within respective Kyoto Encyclopedia of
1185 Genes and Genomes (KEGG) modules: Panel (a): Denitrification (KEGG Module M00529), (b):
1186 Methanogen (M00617), (c): Central Carbohydrate Metabolism (M00001-M00011, M00307-
1187 M00309, M00580, and M00633), (d): Prokaryotic Cytochrome C Oxidase (M00155). Colors
1188 refer to hydrologic treatments: black represents the baseline, brown represents dry conditions,
1189 and dark blue represents wet conditions. Shapes refer to the hydrologic history of the sample: a
1190 square indicates dry, a triangle indicates interim, and a circle indicates wet. The shape fill
1191 represents plant treatment: cross = baseline, open = no plant, closed = plant. Baseline samples
1192 were collected before the initiation of hydrologic and plant treatments. Large, dark, opaque
1193 points represent centroids of samples within a group, while smaller transparent points represent
1194 individual samples. Vectors represent significant ($p \leq 0.1$) relationships among greenhouse gas

1195 fluxes, soil physicochemical factors, and functional gene composition, with the length of the

1196 vectors scaled by the strength of correlation (using the *envfit* function).

Figures

Figure 1

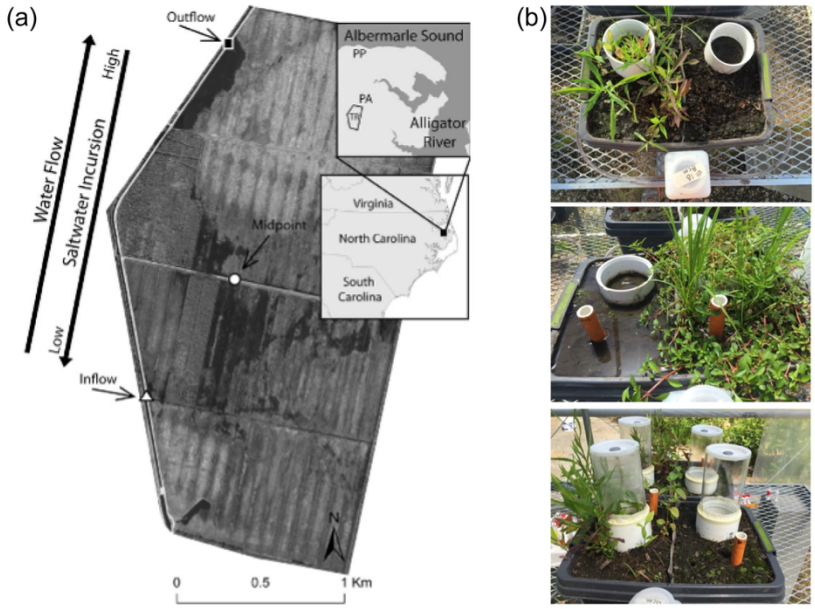

Figure 1. Field site and mesocosm set-up. Wetland mesocosms sourced from the Timberlake Observatory for Wetland Restoration (image modified with permission from Ardón et al., 2013) (a). Aerial view of wetland mesocosm setup, where the left side of the box represents plant treatment, and the right side represents no plant treatment, separated by a stainless mesh divider ((b), top, photo credit: R. Bledsoe). Collars were installed for measuring greenhouse gas concentrations. Also shown is a 1-liter bottle attached to each side of the mesocosm used to maintain water levels. Example of a wet treatment mesocosm with IRIS tubes installed ((b), middle) (photo credit: R. Bledsoe). Example of mesocosm with prepared for GHG sampling ((b), bottom) (photo credit: R. Bledsoe).

Figure 2

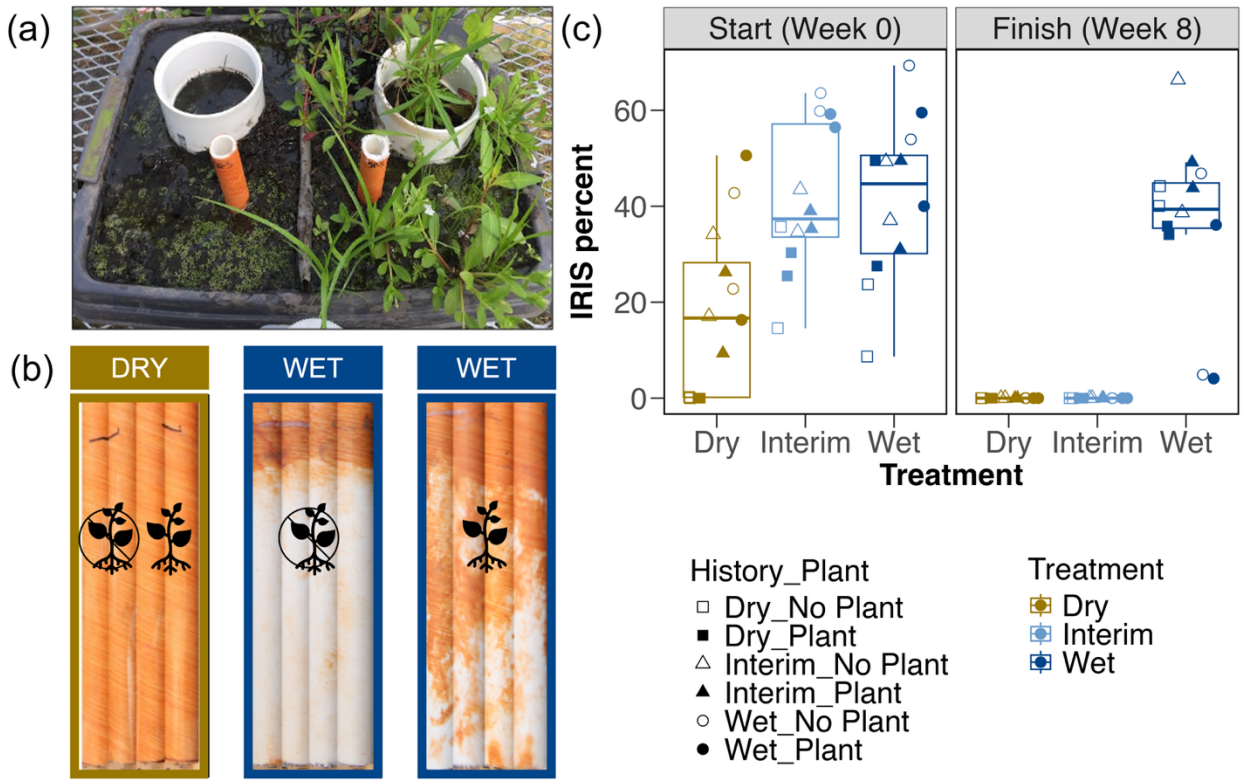

Figure 2. Indicator of reduction in soils (IRIS) tubes mesocosm image (photo credit: R. Bledsoe) (a), IRIS tube example image (photo credit: R. Bledsoe) (b), and boxplots summarizing redox status at the beginning and end of the experiment (c). Percent paint removed from IRIS tubes at the start of the experiment (week 0) and the end of the experiment (week 8). Example IRIS tubes used for ImageJ analysis post-incubation (b) with plant icons crossed out represent IRIS tubes from mesocosms with plants removed, and plant icons represent IRIS tubes from mesocosms with plants present. Box plots summarize percent paint removed from IRIS tubes at start (week 0) and finish (week 8) of experimental incubation. Color represents hydrologic treatment: brown indicates dry, light blue indicates interim, and dark blue indicates wet. Individual samples are plotted as points and colored according to their hydrologic treatment. Point shape represents hydrologic history (square = dry history, triangle = interim history, circle = wet history). Closed points represent mesocosms with plants, while open points represent mesocosms without plants.

Boxplots summarize median, first and third quartiles, and two whiskers extending |≤| 1.5 * interquartile range.

Figure 3

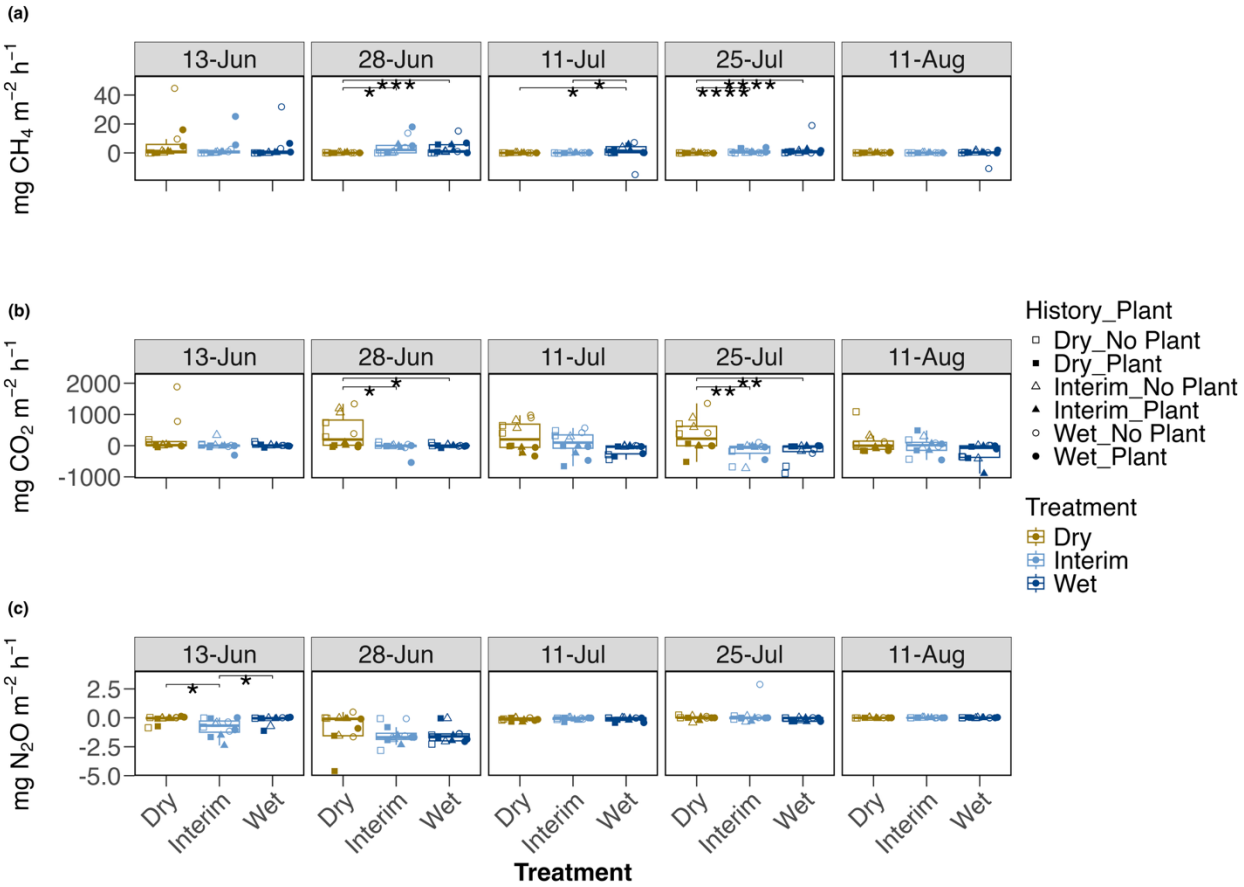

Figure 3. Greenhouse gas fluxes in dry, interim, and wet hydrologic treatments. Fluxes are in milligrams of methane (CH_4) (a), carbon dioxide (CO_2) (b), and nitrous oxide (N_2O) (c) per square meter per hour, and are compared for hydrologic treatments during the five time points. Individual samples are plotted as shapes and colored by hydrologic treatment (brown squares = dry, light blue triangles = interim, dark blue circles = wet). Point shape represents hydrologic history (square = dry history, triangle = interim history, circle = wet history). Closed points represent mesocosms with plants, while open points represent mesocosms without plants. Boxplots summarize the median, first and third quartiles, and two whiskers extending |≤| 1.5 * interquartile range. Asterisks represent significance levels of Dwass, Steel, Critchlow, and Fligner (SDCFlig) tests (****: $p \leq 0.0001$, ***: $p \leq 0.001$, **: $p \leq 0.01$, *: $p \leq 0.05$, no symbol:

$p > 0.05$). An extreme outlier of 248 mg CH_4 m^{-2} h^{-1}, measured in a mesocosm from interim soil history and wet treatment with no plants on July 11th, was used in statistical calculations but not displayed in the plot to improve visualization of differences across treatments.

Figure 4

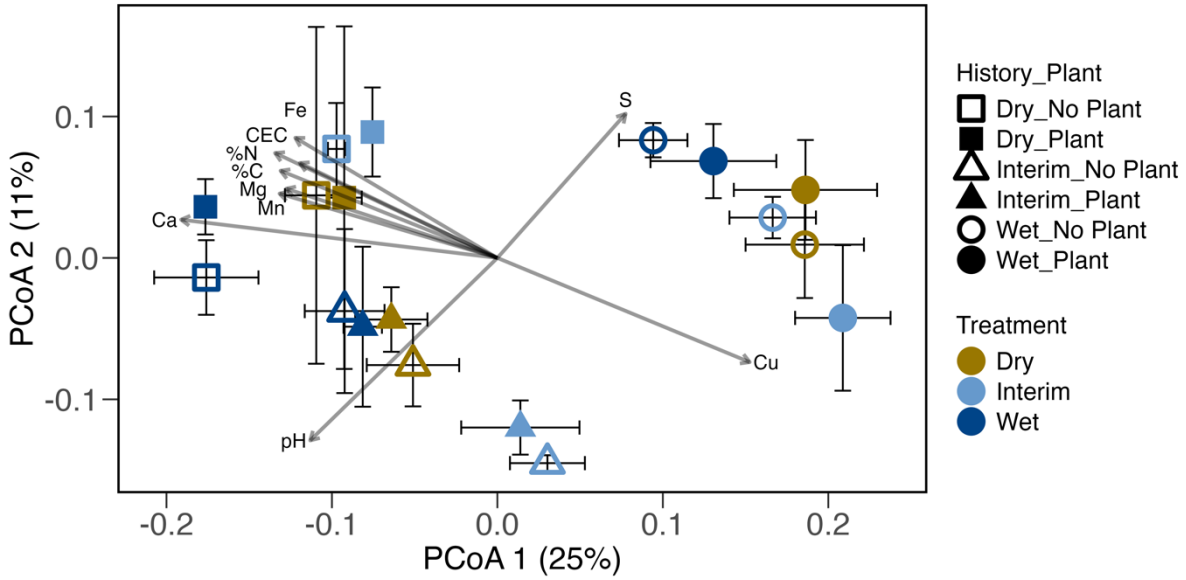

Figure 4. Ordination based on a principal coordinates analysis (PCoA) depicting the composition of the bacterial and archaeal communities based on the 16S rRNA gene. Colors refer to hydrologic treatments: brown indicates dry, light blue indicates interim, and dark blue indicates wet. Shapes refer to the hydrologic history of the sample: a square indicates dry, a triangle indicates interim, and a circle indicates wet. Open shapes refer to samples from mesocosms without plants, while closed shapes refer to samples from mesocosms with plants. Labeled vectors represent relationships among soil physicochemical variables and the microbial community ordination, with $p \leq 0.05$, scaled by their correlation (using the *envfit* function). Abbreviations: CEC: cation exchange capacity.

Figure 5

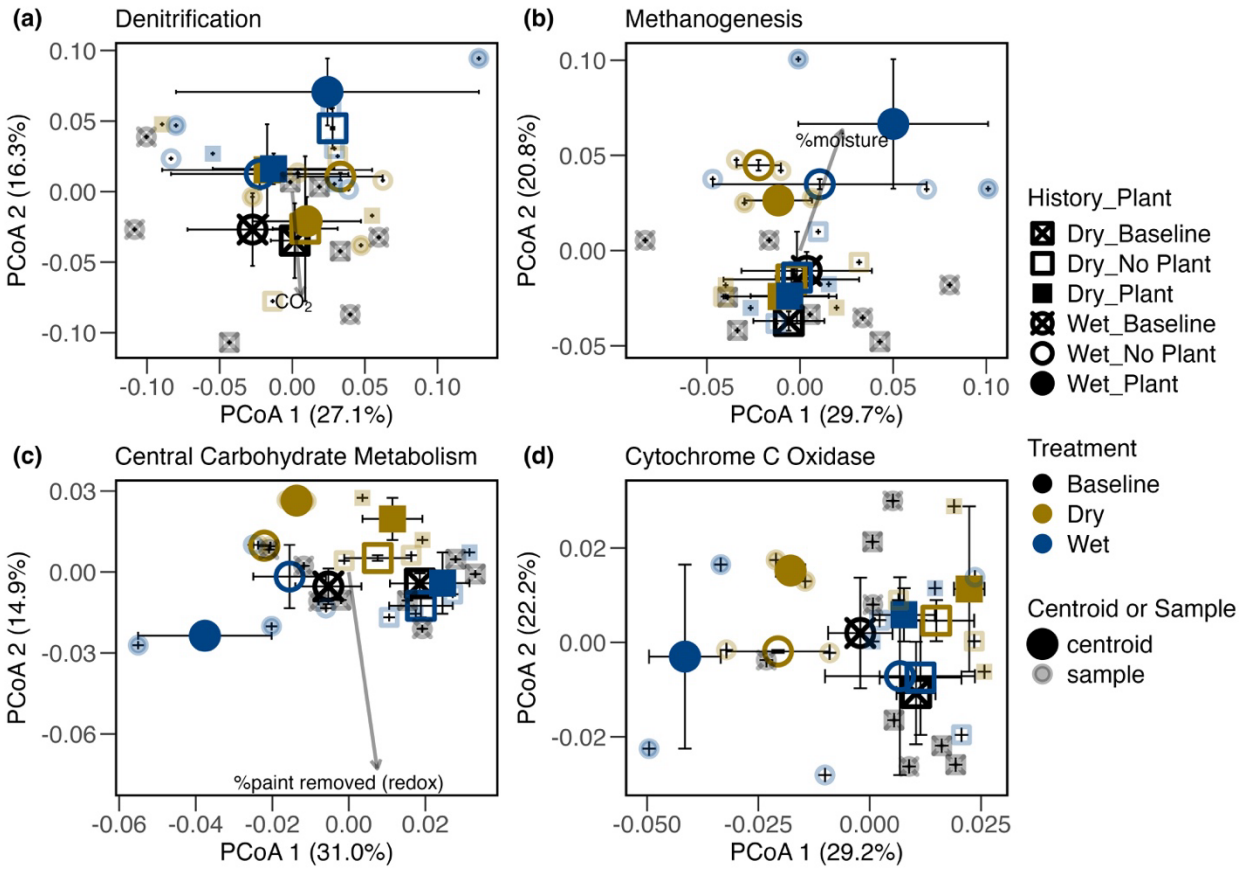

Figure 5. Ordination based on a principal coordinates analysis (PCoA) depicting community composition of the functional gene modules. The PCoA ordination is based on the Bray-Curtis distance of relative abundance of functional genes within respective KEGG modules: Panel (a): Denitrification (KEGG Module M00529), (b): Methanogen (M00617), (c): Central Carbohydrate Metabolism (M00001-M00011, M00307-M00309, M00580, and M00633), (d): Prokaryotic Cytochrome C Oxidase (M00155). Colors refer to hydrologic treatments: black represents the baseline, brown represents dry conditions, and dark blue represents wet conditions. Shapes refer to the hydrologic history of the sample: a square indicates dry, a triangle indicates interim, and a circle indicates wet. The shape fill represents plant treatment: cross = baseline, open = no plant, closed = plant. Baseline samples were collected before the initiation of hydrologic and plant treatments. Large, dark, opaque points represent centroids of samples within a group, while

smaller transparent points represent individual samples. Vectors represent significant ($p \leq 0.1$) relationships among greenhouse gas fluxes, soil physicochemical factors, and functional gene composition, with the length of the vectors scaled by the strength of correlation (using the *envfit* function).